

Microwave Photonics

Jianping Yao, *Senior Member, IEEE, Member, OSA*

(Invited Tutorial)

Abstract—Broadband and low loss capability of photonics has led to an ever-increasing interest in its use for the generation, processing, control and distribution of microwave and millimeter-wave signals for applications such as broadband wireless access networks, sensor networks, radar, satellite communications, instrumentation and warfare systems. In this tutorial, techniques developed in the last few years in microwave photonics are reviewed with an emphasis on the systems architectures for photonic generation and processing of microwave signals, photonic true-time delay beamforming, radio-over-fiber systems, and photonic analog-to-digital conversion. Challenges in system implementation for practical applications and new areas of research in microwave photonics are also discussed.

Index Terms—Injection locking, microwave photonics, optical generation and processing of microwave signals, phase-lock loop (PLL), photonic analog-to-digital conversion, photonic microwave filters, radio-over-fiber, true-time delay.

I. INTRODUCTION

MICROWAVE photonics is an interdisciplinary area that studies the interaction between microwave and optical signals, for applications such as broadband wireless access networks, sensor networks, radar, satellite communications, instrumentation, and warfare systems. In the past few years, there has been an increasing effort in researching new microwave photonics techniques for different applications. The major functions of microwave photonics systems include photonic generation, processing, control and distribution of microwave and millimeter-wave (mm-wave) signals. Many research findings have been reported in the last few years. In general, the topics covered by microwave photonics include photonic generation of microwave and mm-wave signals, photonic processing of microwave and mm-wave signals, optically controlled phased array antennas, radio-over-fiber systems, and photonic analog-to-digital conversion. In this tutorial, techniques developed in the last few years in microwave photonics will be reviewed with an emphasis on the systems architectures for photonic generation and processing of microwave and mm-wave signals, photonic true-time delay beamforming for phased array antennas, radio-over-fiber systems, and photonic

Manuscript received July 01, 2008; revised October 15, 2008. Current version published February 13, 2009. This work was supported by the Natural Sciences and Engineering Research Council of Canada (NSERC).

The author is with the Microwave Photonics Research Laboratory, School of Information Technology and Engineering, University of Ottawa, Ottawa, ON K1N 6N5, Canada (e-mail: jpyao@site.uottawa.ca).

Color versions of one or more of the figures in this paper are available online at <http://www.ieeeexplore.ieee.org>

Digital Object Identifier 10.1109/JLT.2008.2009551

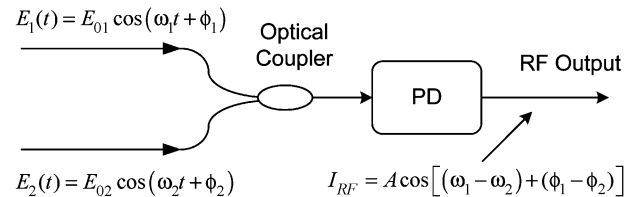


Fig. 1. Optical mixing of two optical waves to generate a microwave or mm-wave signal. PD: photodetector.

analog-to-digital conversion. Challenges in system implementation and new areas of research in microwave photonics are also discussed.

II. OPTICAL GENERATION OF MICROWAVE SIGNALS

A low phase noise and frequency-tunable microwave or mm-wave source is desirable for many applications such as in radar, wireless communications, software defined radio, and modern instrumentation. Conventionally, a microwave or mm-wave signal is generated using electronic circuitry with many stages of frequency doubling to achieve the desired frequency. The system is complicated and costly. In addition, for many applications, the generated microwave or mm-wave signal should be distributed to a remote site. The distribution of a microwave or mm-wave signal in the electrical domain is not practical due to the high loss associated with electrical distribution lines, such as coaxial cable. Thanks to the extremely broad bandwidth and low loss of the state-of-the-art optical fibers, the distribution of a microwave or mm-wave signal over optical fiber is an ideal solution to fulfill this task. Therefore, the ability to generate a microwave or mm-wave signal in the optical domain would allow the distribution of the signal via optical fiber from a central office to a remote site, greatly simplifying the equipment requirement.

Usually, a microwave or mm-wave signal can be generated in the optical domain based on optical heterodyning, in which two optical waves of different wavelengths beat at a photodetector. An electrical beat note is then generated at the output of the photodetector with a frequency corresponding to the wavelength spacing of the two optical waves [1]. Assume that we have two optical waves given by

$$E_1(t) = E_{01} \cos(\omega_1 t + \phi_1) \quad (1)$$

$$E_2(t) = E_{02} \cos(\omega_2 t + \phi_2) \quad (2)$$

where E_{01} , E_{02} are the amplitude terms, ω_1 , ω_2 are the angular frequency terms, and ϕ_1 , ϕ_2 are the phase terms of the two optical waves.

Considering the limited bandwidth of the photodetector, the current at the output of the photodetector is given by

$$I_{\text{RF}} = A \cos[(\omega_1 - \omega_2) + (\phi_1 - \phi_2)] \quad (3)$$

where A is a constant which is determined by E_{01} , E_{02} and the responsivity of the photodetector.

As can be seen from (3), an electrical signal with a frequency equal to the frequency difference of the two optical waves is generated. This technique is capable of generating an electrical signal with a frequency up to THz band, limited only by the bandwidth of the photodetector. However, by beating two optical waves from two free-running laser diodes would lead to a microwave or mm-wave signal with high phase noise since the phases of the two optical waves are not correlated, which will be transferred to the generated microwave or mm-wave signal. Numerous techniques have been proposed and demonstrated in the last few years to generate low-phase-noise microwave or mm-wave signals with the two optical waves being locked in phase. These techniques can be classified into four categories: 1) Optical injection locking, 2) Optical phase-lock loop (OPLL), 3) Microwave generation using external modulation, and 4) Dual-wavelength laser source.

A. Optical Injection Locking

To generate a high-quality microwave or mm-wave signal, the phases of the two optical waves used for heterodyning must be highly coherent. The phase coherence of the two laser diodes can be realized by using optical injection locking [2]. Fig. 2 shows an optical injection locking system that consists of one master laser and two slave lasers. As can be seen an RF reference is applied to the master laser. Due to frequency modulation (FM) at the master laser, an optical carrier and different orders of optical sidebands are generated at the output of the master laser. The signal at the output of the master laser is then injected into the two slave lasers. The two slave lasers are selected such that their free-running wavelengths are close to two sidebands, say the +2nd-order and -2nd-order sidebands in Fig. 2. Therefore, the wavelengths of the two slave lasers are locked to the +2nd-order and -2nd-order sidebands, optical injection locking is thus achieved [2]. Since the two wavelengths from the two slave lasers are phase correlated, the beating of the two wavelengths at a photodetector would generate a beat note with low phase noise. In addition, depending on the design the frequency of the beat note is equal to an integer multiple of the frequency of the RF reference applied to the master laser.

In a simplified version [3], the two slave lasers were replaced by a single multi-longitudinal-mode slave laser with a longitudinal mode spacing of 35 GHz. Again, the master laser is frequency-modulated by an RF reference with a frequency of 5.846 GHz. Two longitudinal modes of the slave laser are thus locked by the +3rd-order and -3rd-order sidebands of the frequency-modulated signal. A beat note at 35-GHz was generated, which was observed by an electrical spectrum analyzer. The 3-dB spectral width of the generated beat note was smaller than the 10-Hz resolution of the spectrum analyzer.

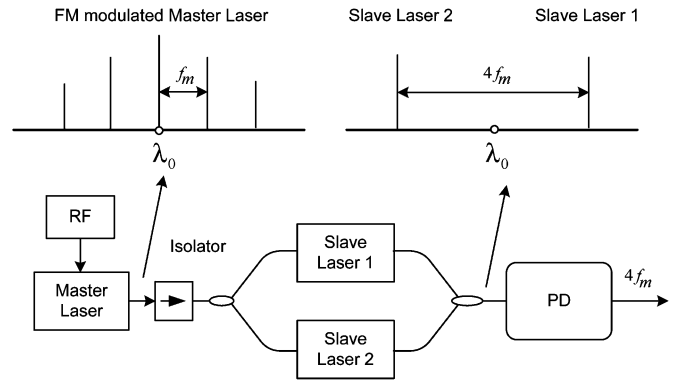


Fig. 2. Optical injection locking of two slave lasers. The master laser is directly modulated by a RF reference with its output injected into the two slave lasers. The slave lasers are wavelength-locked by the +2nd-order and -2nd-order sidebands from the output of the master laser.

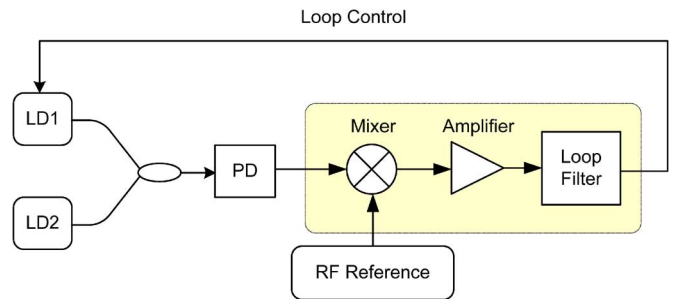


Fig. 3. Schematic of an optical phase lock loop. LD: laser diode. PD: photodetector.

B. Optical Phase Lock Loop

Another approach to achieving phase coherence between two optical waves is to use an optical phase lock loop (OPLL), in which the phase of one laser is actively locked to that of a second laser by an OPLL, as shown in Fig. 3. This technique has been explored extensively in the past few years [4]–[10]. To achieve effective phase locking, the two lasers should be selected to have narrow linewidths and therefore have phase fluctuations only at low frequencies, which would ease significantly the requirement for a very short feedback loop.

As shown in Fig. 3, a beat note is generated at the output of the photodetector. The phase of the beat note is compared with that of an RF reference from a microwave generator at a mixer followed by a low-pass loop filter. The module in the dotted box is an electrical phase detector, with the output voltage being proportional to the phase difference between the beat note and the RF reference, which is an error voltage that is fed back to control the phase of one of the laser source by changing the laser cavity length or the injection current. With a proper feedback loop gain and response time, the relative phase fluctuations between the two lasers are significantly reduced and the phase of the beat note is locked to the RF reference.

It was reported that an OPLL system using two Nd: YAG lasers could generate a microwave signal continuously tunable from 6 to 34 GHz with a linewidth less than 1 mHz [8].

To increase the frequency acquisition capability, a modified OPLL that incorporated a frequency discriminator was proposed [9]. It was demonstrated with the incorporation of the frequency discriminator, a pull-in range as large as 300 MHz was realized.

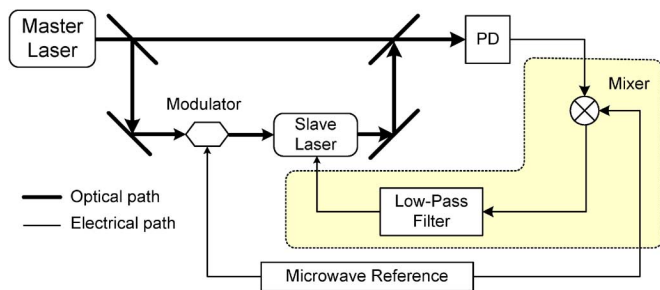


Fig. 4. Diagram showing an optical injection-locking and phase-locking system.

To reduce the feedback frequency, recently an OPLL incorporating a frequency down-conversion module was proposed and demonstrated [10]. The use of the frequency down-conversion module allows the use of lower-frequency components in the phase control module, which would reduce significantly the system cost. In addition, in a discriminator-aided OPLL, the use of the frequency down-conversion module would also allow the use of lower-frequency components in the frequency control module to reduce the system cost [10].

C. Optical Injection Phase Locking

To further improve the signal quality, it was proposed in [11] that the two techniques of optical injection locking and optical phase locking can be combined in a single optical locking system. The diagram of an optical injection-locking and phase-locking system is shown in Fig. 4. The system consists of a master laser, a slave laser, an external modulator, a photodetector, and a phase detection module (dotted box).

As can be seen from Fig. 4, the light from the master laser is divided into two channels, with one channel coupled into the modulator before being injected into the slave laser. The slave laser is locked to one sideband of the modulated signal for optical injection locking of the system. The other channel of the light from the master laser is combined with the output of the slave laser and beat at the photodetector. The beat note is mixed with a microwave reference, with the mixing output filtered by a low-pass filter to achieve phase-locking of the wavelength from the master laser. It was demonstrated experimentally that the proposed system offers lower phase noise compared with the techniques using an injection-locking-only or OPLL-only system.

D. Microwave Generation Based on External Modulation

In addition to the techniques using optical injection locking and OPLL, high-quality microwave signals can also be generated based on external modulation [12]–[15]. A method to generate an mm-wave signal using an external optical modulation technique was first proposed in 1992 [12]. A frequency-doubled electrical signal was optically generated by biasing the Mach-Zehnder modulator to suppress the even-order optical sidebands. A 36-GHz mm-wave signal was generated when the Mach-Zehnder modulator was driven by an 18-GHz microwave signal. Such a system was employed for a remote delivery of video services [13]. In 1994, another method was proposed to generate a frequency-quadrupled electrical signal. Instead of biasing the Mach-Zehnder modulator to suppress the even-order

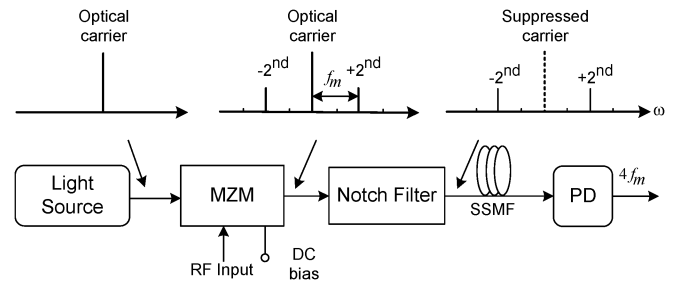


Fig. 5. Microwave signal generation based on external modulation using a Mach-Zehnder modulator and a wavelength-fixed optical filter. MZM: Mach-Zehnder modulator. PD: Photodetector.

optical sidebands, the method [14] was based on the quadratic response of an optical intensity modulator. The optical carrier and the first and third-order optical sidebands were suppressed by adjusting the drive signal level. A 60-GHz millimeter-wave signal was generated when a 15-GHz drive signal was applied to the Mach-Zehnder modulator. However, to ensure a clean spectrum at the output of a photodetector, an imbalanced Mach-Zehnder filter with a free spectral range (FSR) equal to the spacing of the two second-order optical sidebands are used to suppress the unwanted optical spectral components. Recently, an approach using an optical phase modulator to generate a frequency-quadrupled electrical signal was proposed [15]. In this approach, a Fabry-Pérot filter was used to select the two second-order optical sidebands. An electrical signal that has four times the frequency of the electrical drive signal was generated by beating the two second-order sidebands at a photodetector. A key advantage of these approaches in [14], [15] is that an optical modulator with a maximum operating frequency of 15 GHz can generate a millimeter-wave signal up to 60 GHz. However, since both approaches rely on the optical filter to select the two optical sidebands, to generate tunable mm-wave signals a tunable optical filter must be used, which increases significantly the complexity and the cost of the system.

For system applications with frequency reconfigurability, such as wideband surveillance radar, spread-spectrum or software-defined radio, a continuously tunable microwave or mm-wave signal is highly desirable. In [16], [17], two approaches to generating frequency tunable microwave signals using a wavelength-fixed optical filter were demonstrated.

1) *Intensity-Modulator-Based Approach*: Fig. 5 shows a system to generate a continuously tunable mm-wave signal based on external modulation using a Mach-Zehnder modulator and a wavelength-fixed optical filter [16]. The significance of the technique is that no tunable optical filter is required, which simplify significantly the system implementation.

As can be seen from Fig. 5, the system consists of a Mach-Zehnder modulator that is biased at the maximum transmission point of the transfer function to suppress the odd-order optical sidebands. A fiber Bragg grating (FBG) serving as a wavelength-fixed notch filter is then used to filter out the optical carrier. A stable, low-phase noise mm-wave signal that has four times the frequency of the RF drive signal is generated at the output of the photodetector. In the experimental demonstration, a 32 to 50 GHz mm-wave signal was observed on an electrical spectrum analyzer when the electrical drive signal was tuned

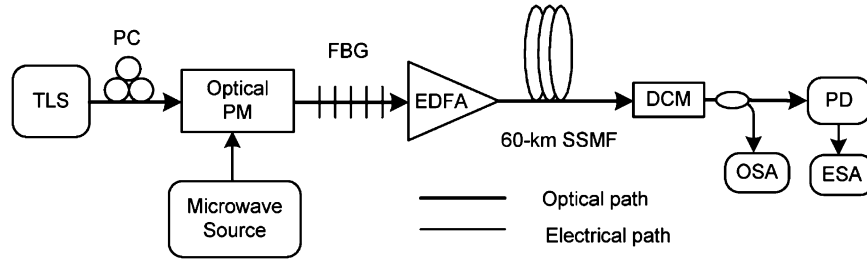


Fig. 6. Microwave signal generation using a phase modulator. TLS: Tunable laser source. DCM: Dispersion compensating fiber. FBG: Fibre Bragg grating. OSA: Optical spectrum analyzer. PC: Polarization controller. PD: Photodetector. PM: Phase modulator. ESA: Electrical spectrum analyzer.

from 8 to 12.5 GHz. The quality of the generated mm-wave signal was maintained after transmission over a 25-km standard single-mode fiber.

2) *Phase-Modulator-Based Approach*: The approach using a Mach-Zehnder modulator to microwave generation, as discussed above, can produce a high-quality frequency-tunable microwave or mm-wave signal with a simple system structure. To suppress the odd- or even-order optical sidebands, however, the Mach-Zehnder modulator should be biased at the minimum or maximum point of the transfer function, which would cause the bias-drifting problem, leading to poor system robustness or a sophisticated control circuit has to be employed to minimize the bias drift.

A simple solution to this problem is to replace the Mach-Zehnder modulator by an optical phase modulator. The key advantage of using an optical phase modulator is that no dc bias is required, which eliminates the bias drifting problem [17]. An experimental setup for the generation of a microwave or mm-wave signal using an optical phase modulator is illustrated in Fig. 6.

The optical carrier from a tunable laser source is sent to the optical phase modulator through a polarization controller (PC). It is different from the use of a Mach-Zehnder modulator, which can be biased to suppress the odd- or even-orders of sidebands, the use of an optical phase modulator will generate all sidebands including the optical carrier. Therefore, a narrow band optical notch filter is used to filter out the optical carrier. In Fig. 6, the optical notch filter is an FBG. In the experiment, the wavelength of the optical carrier was tuned to match the maximum attenuation wavelength of the FBG. The remaining sidebands at the output of the FBG were amplified by an erbium-doped fiber amplifier (EDFA), and then transmitted over single mode fiber. The beat of these optical sidebands at a photodetector generates the required mm-wave signal. It should be noted that the optical sidebands transmitted over the single mode fiber will suffer from the chromatic dispersion of the single mode fiber, which will alter the phase relationship among the sidebands. To maintain the same phase relationship, dispersion compensation is required to eliminate the power fluctuation of the generated electrical signal and to maintain the suppression of the odd-order electrical harmonics when the optical signal is distributed over the single-mode fiber. It was experimentally demonstrated that, when the electrical drive signal was tuned from 18.8–25 GHz, two bands of mm-wave signals from 37.6–50 GHz and from 75.2–100 GHz with high spectral purity were generated locally and remotely.

E. Microwave Generation Using a Dual-Wavelength Laser

Microwave signals can also be generated using a dual wavelength laser source with the two wavelengths separated at a desired frequency [18]. It is different from the techniques of optical injection locking and the OPLL, the two wavelengths from a dual wavelength laser source are not locked in phase. However, due to the fact that the two wavelengths are generated from the same cavity, the phase correlation between the two wavelengths is better than that using two free-running laser sources. The advantage of using a dual-wavelength laser source to generate a microwave or mm-wave signal is that the system is simpler with no need for a microwave reference source, which can reduce significantly the system cost.

Fig. 7(a) shows a dual-wavelength fiber ring laser. To ensure that the two wavelengths are in single-longitudinal mode, a dual-band filter with ultra-narrow passbands must be used, to limit the number of longitudinal mode to be one in each passband. In the experimental demonstration, the ultra-narrow dual-band filter was a dual-wavelength ultra-narrow transmission band FBG with two ultra-narrow transmission bands, which was designed and fabricated based on the equivalent phase-shift (EPS) technique [19]. As can be seen from Fig. 7(b), the two ultra-narrow transmission bands of FBG1 are selected by the two reflection bands of FBG2, with the entire spectral response of the two cascaded FBGs shown in the lower figure of Fig. 7(b). Instead of using an EDFA in the ring cavity, a semiconductor optical amplifier (SOA) was employed as the gain medium. An SOA has less homogeneous line broadening at room temperature, the use of which would reduce significantly the mode competition of the two lasing wavelengths.

The key device was the ultra-narrow band FBG, which was fabricated based on the EPS technique [19]. It is different from the technique with a true phase shift, an equivalent phase-shift is introduced by changing the sampling period of a sampled FBG. In the fabrication of an EPS FBG, the fiber and the phase mask are both fixed, there are less phase fluctuations compared to the true phase shift method, in which the fiber or the phase mask must be laterally shiftable. In addition, the EPS can be controlled more precisely because it only requires a micrometer precision instead of a nanometer precision for true phase shift during the FBG fabrication. Thus, an FBG with more precise phase shift leading to a much narrower transmission bandwidth is possible.

Since the two lasing wavelengths share the same gain cavity, the relative phase fluctuations between the two wavelengths

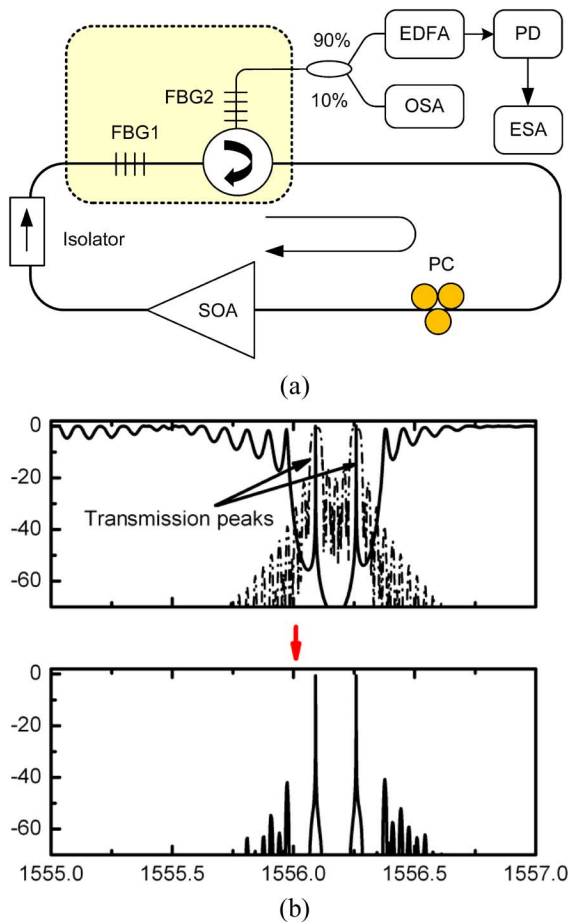


Fig. 7. A dual-wavelength single-longitudinal-mode fiber ring laser for microwave generation. (a) Schematic of the laser, (b) The spectral response of the two cascaded FBGs.

are low. Three dual-wavelength ultranarrow transmission-band FBGs with wavelength spacing of 0.148, 0.33, and 0.053 nm were incorporated into the laser cavity. Microwave signals at 18.68, 40.95, and 6.95 GHz were generated. The spectral width of the generated microwave signals as small as 80 kHz with frequency stability better than 1 MHz in the free-running mode at room temperature was obtained.

III. ALL-OPTICAL MICROWAVE SIGNAL PROCESSING

It was proposed by Wilner and Van den Heuvel [20] that optical fibers could be utilized as delay lines for signal processing, since optical fibers have low loss and large bandwidth.

In the last few years, extensive efforts have been directed to the design and implementation of photonic microwave filters with different architectures to fulfill different functionalities. Fig. 8 shows a diagram of a generic photonic microwave delay-line filter with a finite impulse response (FIR). It consists of a light source, a modulator, a delay-line module, and a photodetector. The key device in a photonic microwave filter is the optical delay-line module, which can be implemented using optical couplers [21]–[23], FBGs [24]–[32], arrayed waveguide (AWG) [33], [34], Mach–Zehnder lattices [35], or a length of dispersive fiber [36], [37].

To avoid optical interference, most of the proposed filters are operating in the incoherent regime. It is known a photonic

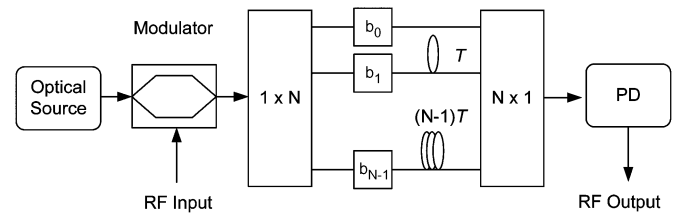


Fig. 8. A diagram showing a generic photonic microwave delay-line filter with a finite impulse response.

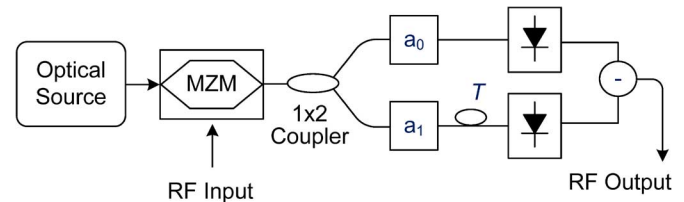


Fig. 9. A photonic microwave delay-line filter with a negative coefficient using differential detection. MZM: Mach–Zehnder modulator.

microwave delay-line filter operating in the incoherent regime would have all-positive tap coefficients. Based on signal processing theory, an all-positive-coefficient microwave delay-line filter would only operate as a low-pass filter. To overcome this limitation, considerable efforts have been taken to design and implement a photonic microwave delay-line filter with negative or complex tap coefficients, to achieve bandpass filtering functionality in the incoherent regime. A comprehensive overview of photonic microwave delay-line filters has been published recently [38], [39]. In this Section, our discussion will be focused only on techniques for the implementation of photonic microwave delay-line filters with negative and complex coefficients.

A. Photonic Microwave Delay-Line Filters With Negative Coefficients

A straightforward way to generate a negative coefficient is to use differential detection [22], [40]. As shown in Fig. 9, the lightwave from an optical source is modulated by a microwave signal, which is then time delayed by optical fiber delay lines with a time delay difference of T . The output signals from the fiber delay lines are fed to a differential photo-detection module, which consists of two matched photodetectors with the detected microwave signals combined and subtracted electrically, leading to the generation of a positive and a negative coefficient. In this approach, the negative coefficient was not generated directly in the optical domain, the filter is not all-optical, but hybrid. The two-tap photonic microwave delay-line filter shown in Fig. 9 can be extended to have multiple taps if the single-wavelength source is replaced by a multiwavelength source and the 3-dB coupler is replaced by a WDM demultiplexer.

A few techniques have been proposed to implement an all-optical photonic microwave delay-line filter with negative coefficients. One approach to generating negative coefficients proposed in 1997 is to use wavelength conversion based on cross-gain modulation in an SOA [41]. As shown in Fig. 10, a tunable laser source operating at λ_1 is modulated by an input microwave signal, and then split into two parts. One part goes through a

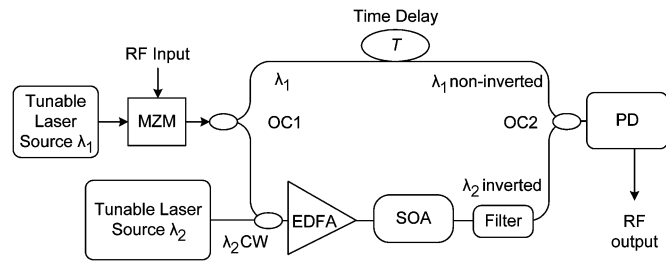


Fig. 10. A photonic microwave delay-line filter with a negative coefficient based on cross-gain modulation in an SOA.

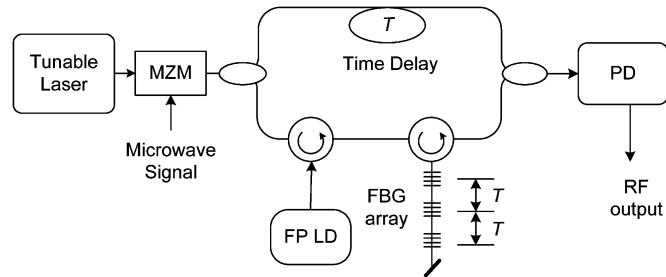


Fig. 11. A photonic microwave delay-line filter with a negative coefficient based on injection-locking of an FP laser diode.

length of optical fiber, to introduce a time delay. The other part is combined with a continuous-wave (CW) lightwave from a DFB laser diode operating at a different wavelength λ_2 , and then fed into an SOA. Due to the cross-gain modulation in the SOA [42], the CW beam λ_2 is also modulated by the input RF signal, but with a π phase inversion compared with the microwave signal carried by λ_1 , leading to the generation of a negative coefficient. An optical bandpass filter is used to filter out the residual λ_1 . Then, the time-delayed microwave signal carried by λ_1 in the upper channel and the π -phase-inverted RF signal carried by λ_2 in the lower channel is combined and detected by a photodetector. A two-tap photonic microwave bandpass filter with one negative coefficient is thus realized. Since the two wavelengths are generated by two independent laser sources, the detection at the photodetector is incoherent. To avoid the beat note between the two wavelengths fall in the passband of the filter, a large wavelength spacing should be chosen. Again, the filter can be extended to be a multi-tap microwave delay-line filter, if the light sources and the two couplers are replaced by multi-wavelength sources, and a WDM demultiplexer and a multiplexer.

A similar approach to generating negative coefficients using an injection-locked Fabry-Perot (FP) laser diode and an FBG array was demonstrated [43]. The filter structure is shown in Fig. 11. Again, the modulated microwave signal is split into two channels. The signal in the upper channel is applied to a photodetector through a delay line. In the lower channel, the signal is injected to an FP laser diode. The FP laser diode is operating with multiple longitudinal modes. One longitudinal mode is locked by the injected optical signal and the other modes that are not locked will experience a cross-intensity modulation. It is similar to the cross-gain modulation in an SOA, the signal modulated on the unlocked modes are with a π phase inversion. As a result, negative coefficients are generated by the unlocked modes. The time delay difference between adjacent unlocked

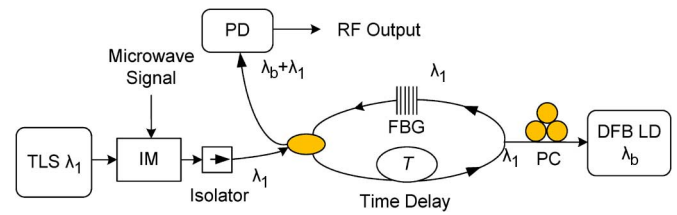


Fig. 12. A photonic microwave delay-line filter with negative coefficients based on carrier depletion effect in a DFB laser diode.

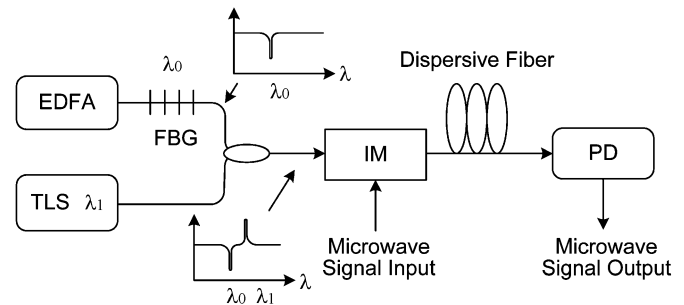


Fig. 13. A photonic microwave delay-line filter implemented using a broadband ASE source cascaded with uniform FBGs to produce negative coefficients.

modes is introduced by an FBG array. The major disadvantage of the technique is the mode competition in the lasing output, which may cause instability of the system. In addition, the mode spacing should be large enough to avoid the beat note between two adjacent modes falling in the passband of the filter.

The use of the carrier depletion effect in a DFB laser diode to generate a negative coefficient was also proposed [44]. A system is shown in Fig. 12. Instead of using a multi-longitudinal mode FP laser diode, a DFB laser diode operating in a single-longitudinal mode is used. The lasing wavelength of the DFB laser diode is injection locked by the injected optical signal. Due to the carrier depletion effect, the microwave signal modulated on the injection carrier is transferred to the lasing wavelength with a π phase inversion, leading to the generation of a negative coefficient. Note that the lasing wavelength of the DFB laser diode should be slight different from the injection wavelength sent to the photodetector through an FBG.

Negative coefficients can also be generated by using an EDFA amplified spontaneous emission (ASE) source cascaded with uniform FBGs [45]. The transmission spectrum at the output of FBGs is altered which is used to generate negative taps. Positive taps are generated by using another multiwavelength source, the output of which is combined with the filtered ASE source. A two-tap delay-line filter with one negative coefficient is shown in Fig. 13.

More recently, a new technique to generate negative coefficients based on two Mach-Zehnder modulators that are biased at complementary transmission slopes was reported [46]. The operation of the microwave phase inversion is shown in Fig. 14. As can be seen, the two Mach-Zehnder modulators are biased at the linear regions of the left and the right slopes of the transfer functions. When a microwave signal is applied to the two modulators, the envelopes of the modulated optical signals are complementary. At the output of a photodetector, two complementary microwave signals are generated, leading to the genera-

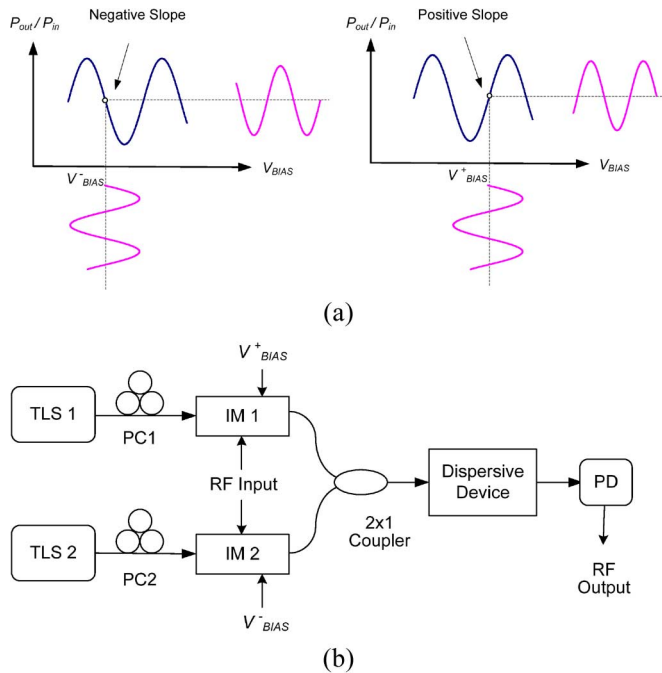


Fig. 14. Photonic microwave delay-line filter with negative coefficients based on phase inversion using complementarily biased intensity modulators. (a) The operation of phase inversion, (b) the schematic of the filter.

tion of a negative coefficient. The time delay difference between two adjacent taps is generated due to the chromatic dispersion of the dispersive device. To implement a microwave delay-line filter with multiple taps, a multi-wavelength laser source or a laser diode array is needed. For those taps with positive and negative coefficients, the corresponding wavelengths must be sent separately to the two Mach-Zehnder modulators. A similar technique using only a single Mach-Zehnder modulator was proposed [47]. Considering the wavelength dependence of the transfer function of the modulator, a proper dc bias would make the modulator operate at the complementary slopes of the transfer functions when the optical wavelengths are at the 1550 nm and 1310 nm windows.

All the filters discussed above are implemented based on the use of one or multiple Mach-Zehnder modulators. Recently, a novel approach to implementing a photonic microwave band-pass filter with negative coefficients based on an optical phase modulator was proposed [48]. The negative coefficients are generated based on phase modulation to intensity modulation (PM-IM) conversion in dispersive elements with complementary dispersions, such as linearly chirped FBGs (LCFBG) with complementary chirps, by reflecting the phase-modulated optical signals from the LCFBGs with positive or negative chirps, microwave signals without or with π phase inversion are generated at the photodetector. An added advantage of using an optical phase modulator is that a phase modulator is not biased, which eliminates the bias drifting problem existing in a Mach-Zehnder modulator. The fundamental concept of the filter operation is shown in Fig. 15(a). An RF signal is applied to the optical phase modulator via the RF port to phase-modulate the multiple wavelengths applied to the phase modulator via the optical port. Since a photodetector functions as an envelope

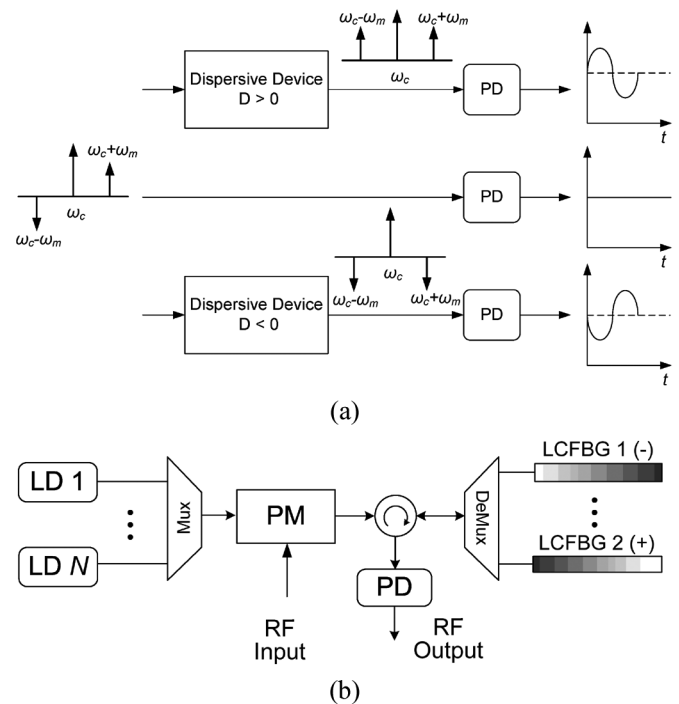


Fig. 15. (a) RF phase inversion based on PM-IM conversion through opposite dispersions. (b) A photonic microwave delay-line filter with a negative coefficient based on PM-IM conversion in two LCFBGs with opposite dispersions.

detector, if a phase-modulated signal is directly applied to a photodetector, no modulating signal will be recovered except a dc. This conclusion can also be explained based on the spectrum of a phase-modulated signal. As shown in Fig. 15(a), a small-signal phase modulated signal has a spectrum with the +1st-order and -1st-order sidebands out of phase. The beating between the optical carrier and the +1st-order sideband exactly cancels the beating between the optical carrier and the -1st-order sideband. However, if the phase-modulated optical signal passes through a dispersive element, the phase relationship between the two sidebands and the optical carrier will be changed, leading to the conversion from phase modulation to intensity modulation. In addition, depending on the sign of the chromatic dispersion, a recovered RF signal with or without a π phase inversion would be obtained, leading to the generation of negative coefficients. The system configuration of the filter is shown in Fig. 15(b).

Instead of using LCFBGs, the PM-IM conversion can also be realized using an optical frequency discriminator, such as a Sagnac loop filter, as shown in Fig. 16 [49]. By locating the optical carriers from the laser sources at the positive or negative slopes of the optical filter spectral response, PM-IM conversion with recovered microwave signals that are in phase or out of phase would be generated, leading to the generation of positive or negative tap coefficients.

Recently, a simple approach to generating negative coefficients in a photonic microwave delay-line filter using a polarization modulator (PolM) was proposed [50], [51]. A PolM is a special optical phase modulator that can support both TE and TM modes, but with opposite phase modulation indices. The operation principle is shown in Fig. 17(a). The lightwave from

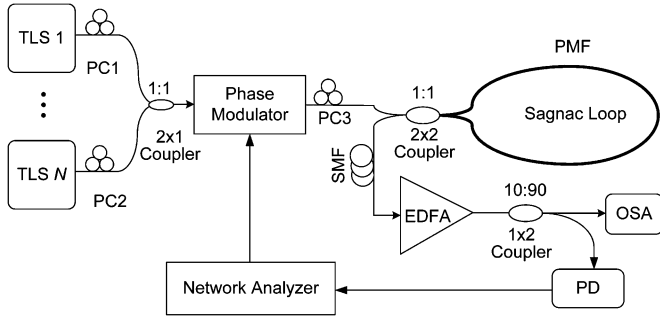


Fig. 16. Photonic microwave delay-line filter with negative coefficients based on PM-IM conversion using optical frequency discriminators.

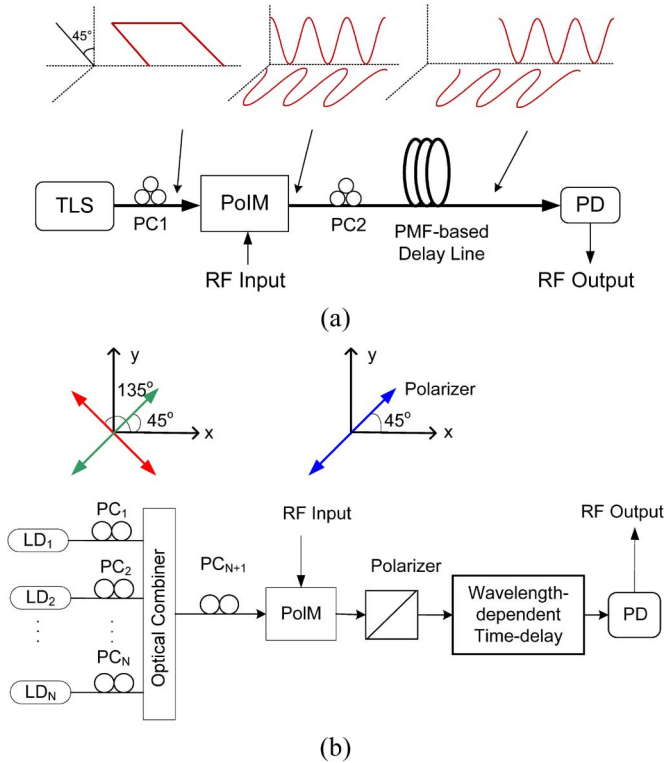


Fig. 17. Photonic microwave delay-line filter with negative coefficients based on a polarization modulator. (a) A photonic microwave delay-line filter based on a PoIM using a single wavelength with time delays generated by a section or two sections of PMF. (b) A photonic microwave delay-line filter based on a PoIM using N wavelengths with arbitrary number of taps and arbitrary tap coefficients.

a tunable laser source is sent to a PoIM via a polarization controller with its polarization direction aligned to have a 45° with respect to one principal axis of the PoIM, which is modulated by an input RF signal. Thanks to the polarization modulation at the PoIM, two complementary RF signals carried by two optical carriers with identical wavelengths but orthogonal polarizations are achieved at the output of the PoIM. The optical microwave signals are fed into a section or two sections of polarization maintaining fiber (PMF) to serve as a delay-line with two or four time delays. A photonic microwave bandpass filter of two or four taps with one or two negative coefficients was experimentally demonstrated [50].

To implement a photonic microwave delay-line filter with arbitrary number of taps and arbitrary tap coefficients, a modified structure based on a PoIM was recently proposed, as

shown in Fig. 17(b) [51]. Instead of using a single-wavelength light source, to achieve a microwave delay-line filter with N taps, a light source with N wavelengths or laser array with N laser diodes are needed. An optical polarizer is connected at the output of the PoIM with its transmission axis aligned at an angle of 45° to one principal axis of the PoIM. By adjusting the polarization directions of the input lightwaves to be 45° or 135° to one principal axis of the PoIM, an in-phase or out-of-phase intensity-modulated optical microwave signal is obtained at the output of the optical polarizer, leading to the generation of negative or positive coefficients. A time-delay difference between adjacent taps is generated by using a wavelength-dependent delay line, such as a dispersive fiber or a chirped FBG.

B. Photonic Microwave Delay-Line Filters With Complex Coefficients

The tunability of a photonic microwave delay-line filter is usually achieved by adjusting the time-delay difference. However, the change of the time-delay difference would lead to the change of the free spectral range (FSR), which results in the change of the 3-dB bandwidth as well as the entire shape of the filter frequency response. For many applications, it is highly desirable that only the center frequency of the passband or stopband is changed while maintaining the shape of the frequency response unchanged. A solution to this problem is to design a photonic microwave delay-line filter with complex coefficients.

An N -tap microwave delay-line filter with complex coefficients should have a transfer function given by

$$\begin{aligned} H(\omega) &= a_0 + a_1 e^{-j\theta} \cdot e^{-j\omega T} + \dots \\ &\quad + a_{N-1} e^{-j(N-1)\theta} \cdot e^{-j\omega(N-1)T} \\ &= \sum_{n=0}^{N-1} a_n e^{-jn\theta} \cdot e^{-j\omega n T} \end{aligned} \quad (4)$$

where T is the time delay different between two adjacent taps. To tune the filter while maintaining the shape of the frequency response, the phase shifts of all the taps should maintain a fixed relationship, as can be seen from (4). Therefore, the phase shift of each tap should be tuned independently.

Three photonic microwave delay-line filter architectures with complex coefficients have been recently reported [52]–[54]. In [52], a two-tap photonic microwave delay-line filter with one complex coefficient was implemented using a system consisting of three optical attenuators and two microwave couplers. Specifically, we expect the filter to have a transfer function given by

$$H(f) = \cos(2\pi f T + \varphi) \quad (5)$$

where T is a constant. By tuning the phase φ , the filter transfer function will be shifted laterally along the horizontal direction without changing the shape. Equation (5) can be rewritten as

$$\begin{aligned} H(f) &= \frac{a}{2}(e^{j\omega T} + e^{-j\omega T}) - \frac{b}{2j}(e^{j\omega T} - e^{-j\omega T}) \\ &= e^{-j\omega T} \left\{ \frac{a}{2}(e^{j\omega 2T} + 1) - \frac{b}{2j}(e^{j\omega 2T} - 1) \right\} \end{aligned} \quad (6)$$

where $a = \cos(\varphi)$, $b = \sin(\varphi)$. As can be seen the filter has one complex coefficient $-b/2j$. The term $e^{-j\omega T}$ only introduces a

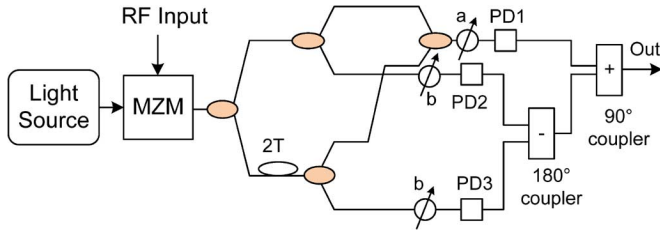


Fig. 18. A two-tap photonic microwave filter with a complex coefficient using three optical attenuators and two microwave couplers.

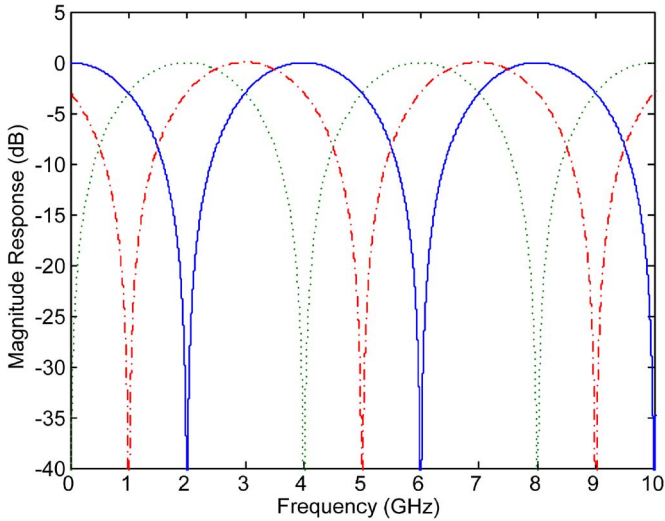


Fig. 19. Frequency response of a photonic microwave delay-line filter with a complex coefficient. Solid: $a = 1, b = 0$; dotted: $a = 0, b = 1$; dash-dot: $a = b = 0.71$.

linear phase, which will not affect the shape of the filter spectral response.

As can be seen from (6), the filter can be realized by a system shown in Fig. 18. By changing the values of a and b through tuning the attenuations of the variable attenuators, the frequency response of the filter is laterally shifted, while the FSR and the 3-dB bandwidth are maintained unchanged, as can be seen from Fig. 19. Since the values of a and b are changed by using the optical attenuators, the tuning range of a and b is from 0 to 1, which limits the RF phase shift from 0 to 180° or a tunable range of a half FSR. We should note that the complex coefficient is generated in the electrical domain after the photodetectors, the system is not all-optical, but hybrid.

An all-optical tunable photonic microwave delay-line filter with a complex coefficient was recently proposed and demonstrated [53]. The complex coefficient was generated by changing the phase of the RF signal, which was realized based on a combined use of optical single-sideband modulation (SSB) and stimulated Brillouin scattering (SBS). The experimental setup is shown in Fig. 20. It was demonstrated that the phase of a microwave signal carried by an optical carrier will experience microwave phase shift if the spectrum of the optical carrier or the sideband is falling in the SBS gain spectrum when passing through an optical fiber in which an SBS is resulted [55].

Since the generation of a complex coefficient involves the use of an EDFA, an additional Mach-Zehnder modulator, and a

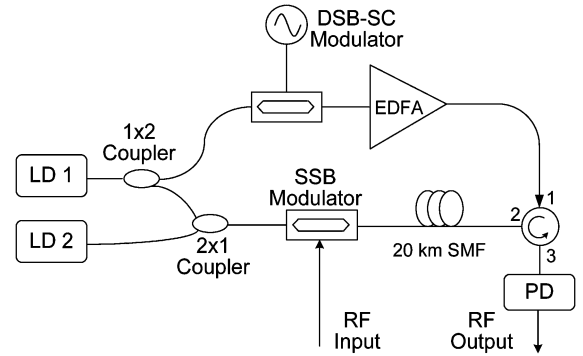


Fig. 20. A two-tap photonic microwave delay-line filter with a complex coefficient based on SSB modulation and SBS.

long fiber (20 km in the experiment), to implement a multi-tap filter the system will be extremely complicated, highly power consuming, and costly. A simpler system architecture for a tunable photonic microwave delay-line filter with complex coefficients was recently demonstrated [54]. The complex coefficient is generated using a wideband tunable optical RF phase shifter that consists of two electro-optic Mach-Zehnder modulators, shown in Fig. 21(a). The phase of the RF signal is shifted by simply adjusting the bias voltages applied to the two electro-optic Mach-Zehnder modulators, and the phase shift remains constant over the microwave spectral region of interest. Fig. 21(b) shows the measured phase shifts for different bias voltages over a large microwave frequency band. As can be seen the phase shifts are independent of the microwave frequency.

C. Nonuniformly Spaced Photonic Microwave Delay-Line Filters

The filters in [52]–[54] with complex coefficients have the potential to be extended to have multiple taps, but the filter complexity would be significantly increased. To design a photonic microwave delay-line filter with complex coefficients having a simple structure, we have recently developed a new concept by generating complex coefficients based on a delay-line architecture with nonuniformly spaced taps. It was demonstrated that the complex coefficients can be equivalently generated by introducing additional time delays to the taps [56].

It is known that a regular, uniformly-spaced microwave delay-line filter has an impulse response $h_R(t)$ given by

$$h_R(t) = \sum_{k=0}^{N-1} \alpha_k \delta(t - kT) \quad (7)$$

where N is the number of taps, α_k is the filter coefficient of the k th tap, $T = 2\pi/\Omega$ is the time delay difference between two adjacent taps, and Ω is the FSR of the filter. Apply the Fourier Transform to (7), we have the frequency response of the filter,

$$H_R(\omega) = \sum_{k=0}^{N-1} \alpha_k \exp\left(-jk \frac{2\pi}{\Omega} \omega\right). \quad (8)$$

It is known that $H_R(\omega)$ has a multi-channel frequency response with adjacent channels separated by an FSR, with the

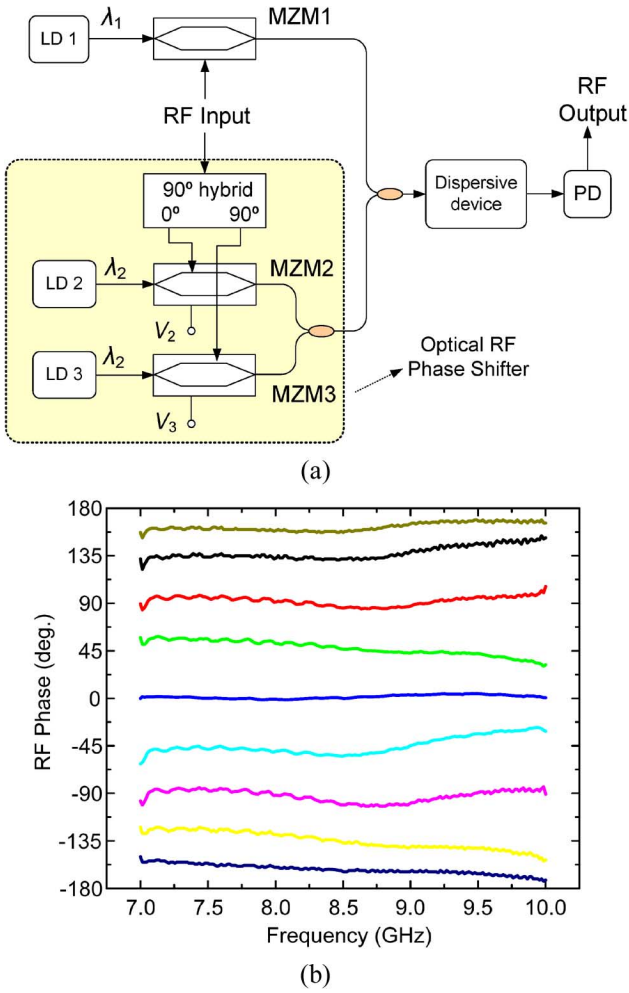


Fig. 21. A photonic microwave delay-line filter with a complex coefficient generated based on an optical RF phase shifter. (a) The system architecture. (b) The measured phase shifts for different bias voltages over a large microwave frequency band. The phase shifts are independent of the microwave frequency.

m th channel located at $\omega = m\Omega$. Note that except for the different central frequencies, the frequency responses for all the channels are exactly identical.

In a regular photonic microwave delay-line filter based on incoherent detection, the coefficients are usually all positive, or special designs have to be incorporated to generate negative or complex coefficients, as discussed earlier in this section. However, a phase term can be introduced to a specific coefficient by adding an additional time delay at the specific tap, which is termed time-delay-based phase shift [56]. For example, at $\omega = m\Omega$ a time delay shift of $\Delta\tau$ will generate a phase shift given by $\Delta\varphi = -\Delta\tau \times m\Omega$. Note that such a phase shift is frequency-dependent, which is accurate only for the frequency at $m\Omega$, but approximately accurate for a narrow frequency band at around $m\Omega$. For most of applications, the filter is designed to have a very narrow frequency band. Therefore, for the frequency band of interest, the phase shift can be considered constant over the entire bandwidth. As a result, if the m th bandpass response, where $m \neq 0$, is considered, one can then achieve the desired phase shift at the k th tap by adjusting the time delay shift by $\Delta\tau_k$. Considering the time delay shift of $\Delta\tau_k$, one can get the

frequency response of the nonuniformly-spaced delay-line filter at around $\omega = m\Omega$,

$$\begin{aligned} H_N(\omega) &= \sum_{k=0}^{N-1} \alpha_k \exp \left[-j \left(k \frac{2\pi}{\Omega} + \Delta\tau_k \right) \omega \right] \\ &= \sum_{k=0}^{N-1} \alpha_k \exp(-j\omega\Delta\tau_k) \times \exp \left(-jk \frac{2\pi}{\Omega} \omega \right) \\ &\approx \sum_{k=0}^{N-1} [\alpha_k \exp(-jm\Omega\Delta\tau_k)] \times \exp \left(-jk \frac{2\pi}{\Omega} \omega \right). \quad (9) \end{aligned}$$

As can be seen from (9), one can get an equivalent phase shift for each tap coefficient. Specifically, if the desired phase shift for the k th tap is φ_k , the total time delay τ_k for the k th tap is $\tau_k = kT - \varphi_k/m\Omega$. As a result, if the time delay of each tap is adjusted, the filter coefficients would have the required phase shifts to generate the required passband with the desired bandpass characteristics.

A seven-tap photonic microwave delay-line filter with nonuniformly-spaced taps to produce a flat-top bandpass frequency response was designed and experimentally demonstrated [56]. The experimental setup is shown in Fig. 22(a). Assume that the passband of interest is at $m = 1$ and the frequency response of the bandpass has a shape of a rectangle, then the corresponding impulse response should be a *Sinc* function, which has both positive and negative values extending to infinity along the horizontal axis. For practical implementation, the calculated impulse response should be cut off to enable a physically realizable filter. If a regular photonic microwave delay-line filter is employed to produce the frequency response, the filter coefficients can be selected to be $[-0.12, 0, 0.64, 1, 0.64, 0, -0.12]$. The frequency response is shown as dotted line in Fig. 22(b), where $T = 82.6$ ps, which corresponds to an FSR of 12.1 GHz. The 3-dB bandwidth of the filter is 5.0 GHz with a central frequency of 12.1 GHz.

With the proposed technique, the same bandpass characteristics at $m = 1$ can be generated by using nonuniform spacing. The filter was designed having all-positive coefficients of $[0.12, 0, 0.64, 1, 0.64, 0, 0.12]$. The time delays for the seven taps are then $[-2.5T, -2T, -T, 0, T, 2T, 2.5T]$, with the taps nonuniformly spaced. Since at $m = 0$, there is no phase shifts introduced to the taps, there is always a baseband resonance which was eliminated by using an optical phase modulator in the system. It is known the PM-IM conversion in a dispersive fiber would produce a frequency response with a notch at dc [57], [58]. The frequency response of the PM-IM conversion is designed to make its first peak be located at $f = 12.1$ GHz, which is shown as the dash-dot line in Fig. 22(b). The overall frequency response of the nonuniformly-spaced filter is calculated and shown as solid line in Fig. 22(b). It is clearly seen a flap-top frequency response is achieved in a photonic microwave delay-line filter with all-positive coefficients. The 3-dB bandwidth was 4.9 GHz and the central frequency was 12.1 GHz. The frequency response of the passband is close to that generated by a regular photonic microwave delay-line filter with true negative taps.

As we mentioned earlier the time-delay-based phase shift is frequency dependent. As a result, the phase shifts due to

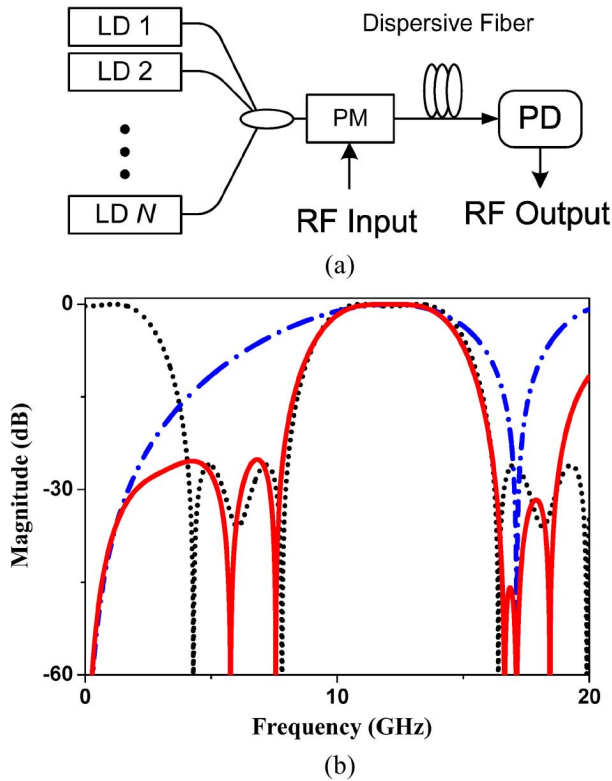


Fig. 22. (a) A nonuniformly-spaced photonic microwave delay-line filter. (b) Dotted line: the frequency response of a regular photonic microwave delay-line filter with true positive and negative coefficients. Dash-dot line: the frequency response of the PM-IM conversion. Solid line: the frequency response of the nonuniformly-spaced photonic microwave delay-line filter.

the additional time delays would be different for different passbands. Therefore, in a nonuniformly-spaced photonic microwave delay-line filter, the frequency responses for different channels are different. In addition, within the m th passband, the time-delay-based phase shift is accurate only for the frequency at $m\Omega$, and approximately accurate for a narrow band at around $m\Omega$. The maximum error of the phase shift is determined by the maximum bandwidth of the bandpass concerned and the central frequency. For many applications, it is usually required that the bandwidth of the passband is very narrow, then the errors due to the frequency-dependent phase shift are small and negligible, which ensures the effectiveness of the proposed technique.

The proposed technique to design a nonuniformly spaced microwave delay-line filter is particularly useful for applications such as arbitrary microwave waveform generation. Recently, we have applied the same concept to introduce phase shifts to an RF pulse to implement RF pulse phase encoding [59]. We have also designed and implemented a nonuniformly spaced microwave delay-line filter with a quadratic phase response for chirped microwave pulse generation [60].

D. Optical Mixing of Microwave Signals

In an optical microwave signal processor, in addition to the functionality of microwave filtering, optical microwave mixing is another important functionality which can find applications in radio-over-fiber systems and other microwave systems for microwave frequency up- or down-conversion. Different mixing architectures have been summarized in [61]. In this subsection,

we will give a brief introduction to optical microwave mixing and then a few examples demonstrated recently will be provided.

Fig. 23 shows three different optical microwave mixing architectures. The architecture shown in Fig. 23(a) combines direct modulation of an RF signal at a laser diode with an external modulation of a local oscillator (LO) signal at a Mach-Zehnder modulator. If the LO frequency is not too high, the system can be simplified, as shown in Fig. 23(b), in which both the RF signal and the LO signal are combined and sent to a laser diode. Due to the chirping at the laser diode, the output signal is frequency modulated. The use of an unbalance Mach-Zehnder (UMZ) interferometer, by locating the optical carrier at one slope of the spectral response, frequency-modulation to intensity-modulation (FM-IM) conversion is realized. The UMZ interferometer can also be replaced by an FBG. To increase the dynamic range, the FBG should be designed to maximize the linear region of the slope. In addition, by locating the optical carrier at a point closer to the bottom of the FBG spectral response, the dynamic range can also be improved since the optical carrier-induced noise at the photodetector can be significantly reduced, leading to an increased spurious-free dynamic range (SFDR) [62], [63]. For some applications, both the RF signal frequency and the LO frequency are high. In this case, the mixing has to be implemented at an external modulator, by combining the RF signal and the LO using a microwave combiner and then apply to the external modulator. One concern in using an optical system for microwave mixing is the existence of many unwanted frequency components, which are usually eliminated in the electrical domain using a microwave filter. To implement an all-optical microwave mixer, both the mixing and bandpass filtering have to be realized in the optical domain. Recently, we proposed an approach that functions simultaneously as an all-optical microwave mixer and an all-optical microwave bandpass filter [64]. The schematic of the system is shown in Fig. 24.

The architecture is similar to that shown in Fig. 23(c), except that the modulator is an optical phase modulator and the light source is a multi-wavelength source. The microwave mixing and filtering functions are simultaneously implemented. The mixing operation is done in the phase modulator, to which a large LO signal is applied to make the phase modulator operating in the nonlinear region, leading to the generation of different mixing spectral components. The filtering operation is realized thanks to the use of a multi-wavelength source. If the number of wavelength is N , the system is an N -tap microwave delay-line filter. Considering that the PM-IM conversion at a dispersive fiber will generate a notch at dc, the overall frequency response of the system is a bandpass filter with baseband resonance eliminated by the notch at dc [57], [58]. Therefore, the entire system is functioning as a microwave mixer and a bandpass filter. By properly designing the filter to make the central frequency of the passband locate at the frequency of interest, an up- or down-converted microwave signal free of other frequency components is obtained.

An experiment was performed to achieve microwave frequency up-conversion from 3 to 11.8 GHz [64]. In the experimental setup, a fiber ring laser with 30 wavelengths and a wavelength spacing of 0.2 nm was used as the multiwavelength

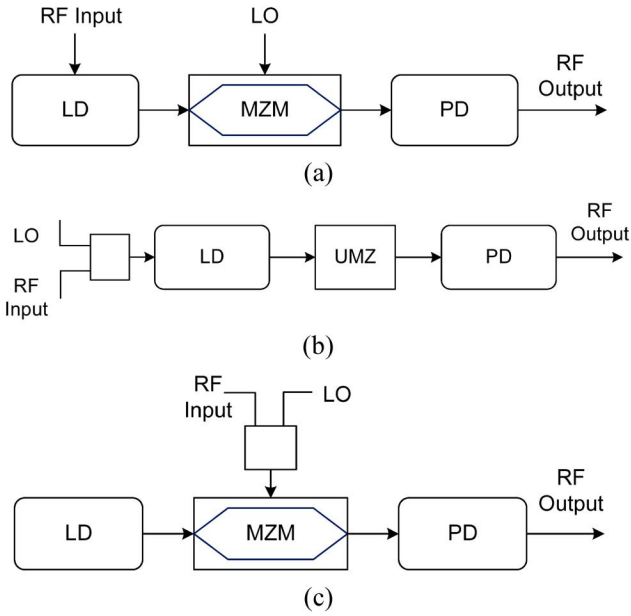


Fig. 23. Architectures for all-optical microwave mixing. (a) Optical mixing that combines direct modulation and external modulation, (b) Optical microwave mixing based on direct modulation at a laser diode with a unbalanced interferometer to perform FM-IM conversion, (c) Optical microwave mixing based on external modulation.

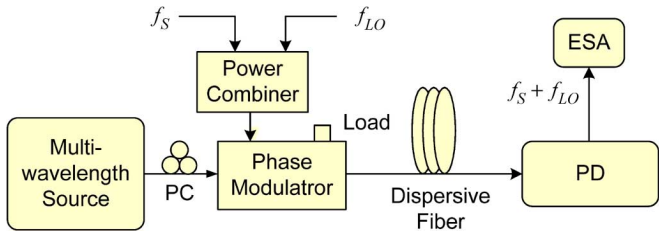


Fig. 24. An all-optical microwave signal processor that functions simultaneously as an all-optical mixer and a bandpass filter.

source [65]. The dispersive fiber was a single mode fiber. Considering a wavelength spacing of 0.2 nm, a length of 25-km standard single-mode fiber would lead to a frequency response with the central frequency of the passband locate at 11.8 GHz. Therefore, the up-converted microwave component at 11.8 GHz would be selected. Fig. 25 shows the experimental results of the mixing output, with and without filtering operation. Fig. 25(a) shows the spectrum of the mixing components when the light source was a single wavelength source, with no bandpass filtering operation. All frequency components were observed. Fig. 25(b) shows the spectrum when the 30-wavelength laser source was used. The system was operating as a bandpass filter. The up-converted frequency component at 11.8 GHz was selected with other components being eliminated.

The use of a phase modulator for optical microwave mixing to study the system performance with data transmission has been investigated in [66], [67].

IV. PHOTONIC TRUE-TIME DELAY BEAMFORMING

Phased array antennas (PAA) are playing an important role in modern radar and wireless communication systems. Conventional phased array antennas are realized based on electrical phase shifters, which suffer from the well-known beam squint

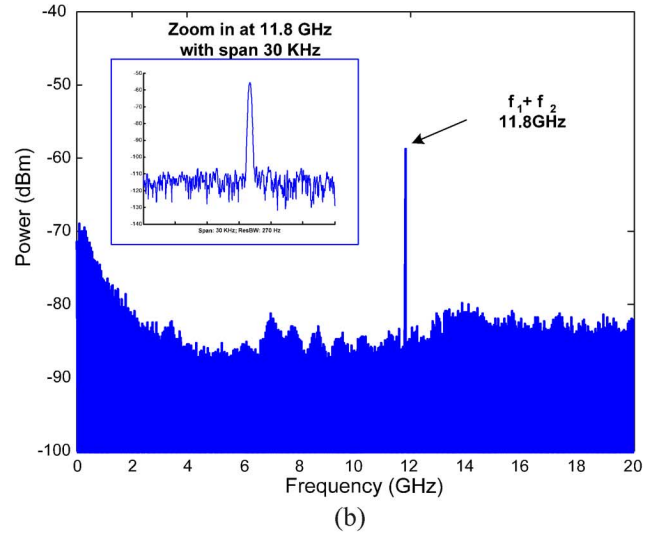
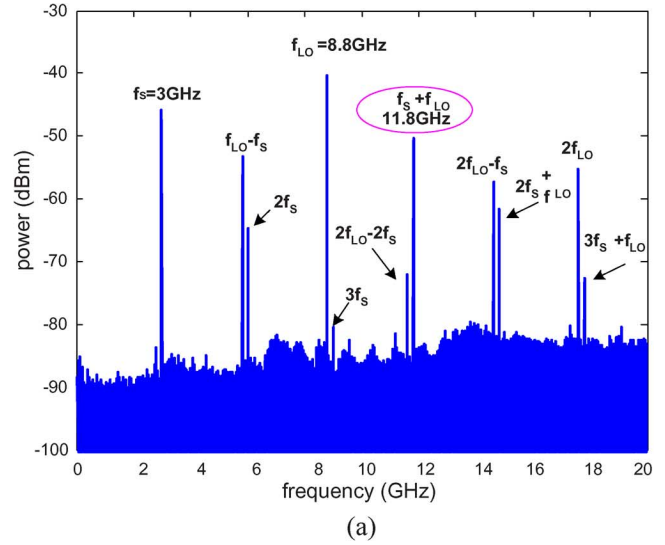


Fig. 25. Power spectra at the output of the photodetector. (a) Different spectral components are observed if a single wavelength source is used. (b) When a multi-wavelength source with over 30 wavelengths is used, the system is also a microwave passband filter. Only the up-converted signal at 11.8 GHz is obtained and other frequency components are rejected.

problem, limiting the phase array antennas for narrowband operations. For many applications, however, it is highly desirable that the phase array antennas can operate in a broad band. An effective solution to the problem is to use true-time delay beam-forming.

A. Squint Phenomenon

The squint phenomenon is characterized by the position of the mainlobe of the array factor being oriented at different angles for different microwave signal frequencies. In other words, the energy associated with different frequencies is oriented in different directions and thus restricts the use of the antenna for narrowband applications only.

As can be seen from Fig. 26(a), to steer the beam to a direction with angle of θ with respect to the broadside direction, a phase shifter with a phase shift of $\Delta\phi$ is required,

$$\Delta\phi = 2\pi \frac{\Delta L}{\lambda} = 2\pi \frac{d \sin \theta}{\lambda}. \quad (10)$$

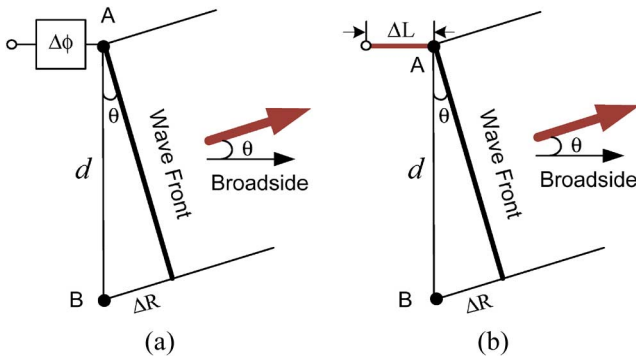


Fig. 26. (a) Beam steering using a phase shifter. (b) Beam steering using a delay line.

The beam pointing direction is then given by

$$\theta = \sin^{-1} \frac{\Delta\phi\lambda}{2\pi d}. \quad (11)$$

As can be seen the beam pointing direction is a function of the microwave wavelength or frequency. Therefore, a beamforming system using electrical phase shifters will only operate for narrowband signals or the beam will be corrupted, a phenomenon called beam squint. The problem can be solved if the phase shifter is replaced by a delay line, as shown in Fig. 26(b), where a delay line with a length of $\Delta L = d \sin \theta$ is used. The beam pointing direction is now given by

$$\theta = \sin^{-1} \frac{\Delta L}{d}. \quad (12)$$

It can be seen that the beam pointing direction is independent of the microwave frequency. A wide instantaneous bandwidth operation that is squint free would be ensured.

Fig. 27 gives an example of an antenna of six elements separated by a distance of 1 cm ($d = \lambda_0/2$) operating at a central frequency f_0 of 15 GHz. For the purposes of illustrating the beam squint effect, the bandwidth of the antenna will be assumed to be 10 GHz. Thus, the behavior of the antenna will be studied for the frequencies from 10 to 20 GHz. The far-field radiation pattern of the array factor (considering isotropic elements) for the central frequency f_0 is given in Fig. 27.

Fig. 28 illustrates the far-field radiation pattern of the array factor for frequencies between 10 and 20 GHz by an interval of 1 GHz. From Fig. 28, one can clearly see that the orientation of the mainlobe varies with the feed signal frequency. This phenomenon decreases significantly the performance of the system.

To eliminate the beam squint, a solution is to use true-time delay. This method consists of introducing a time delay progression to the feed signals instead of a phase progression. This time delay is constant for all frequencies and thus translates into a variable phase shift with respect to frequency. Fig. 29 shows the array factor by using the same phased array antenna example as for the conventional phase shifters ($N = 6$ elements separated by a distance of 1 cm) operating at the same central frequency f_0 of 15 GHz. The behavior of the antenna is studied for the frequencies from 10 to 20 GHz. This time, true-time delays component are used instead of conventional phase shifters. These elements introduce a time progression of 16.67 ps which corresponds to the same phase of $\pi/2$ at a frequency of 15 GHz.

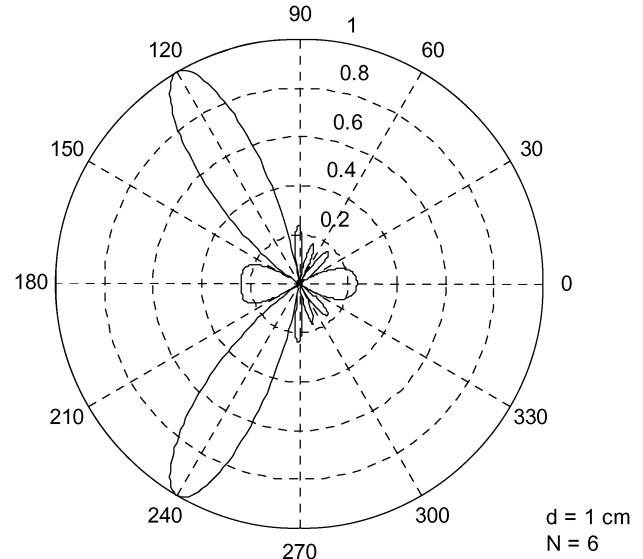


Fig. 27. Array factor for a phased array antenna of six elements with $d = \lambda_0/2$ at $f_0 = 15$ GHz.

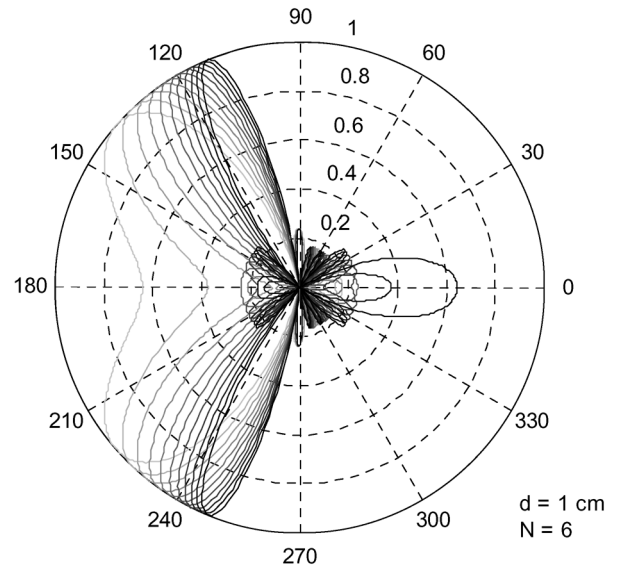


Fig. 28. Beam squint effect for a phased array antenna using electrical phase shifters operating at frequencies between 10–20 GHz.

Fig. 29 illustrates the far-field radiation pattern of the array factor for frequencies between 10 and 20 GHz by an interval of 1 GHz which uses true-time delay components. Fig. 29 clearly shows that the orientation of the mainlobe does not vary with the feed signal frequency.

B. Photonic True-Time Delay Beamforming

Traditionally, feed networks and phase shifters for phased array antennas were realized using electronic components. This was the most intuitive approach since antennas operate on an electrical driving source. With the advancement of technology, severe limitations were observed in electrical devices. For example, copper wires display high losses at high frequencies resulting in a limited bandwidth for the feed signals. Furthermore, electrical beamforming networks have a relatively high weight, thus limiting their use in airborne systems.

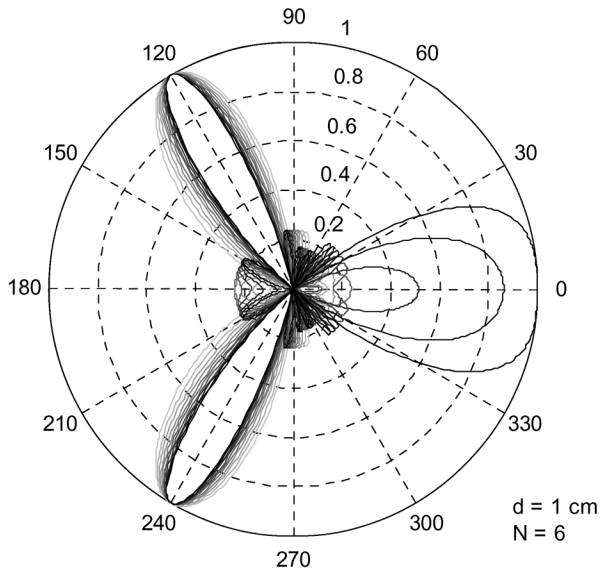


Fig. 29. Array factor of a phased array antenna using true-time delay components operating at frequencies between 10–20 GHz.

Optical components, with key advantages such as immunity to electromagnetic interference, low loss, small size and light weight are being considered as a promising alternative for wide-band phased array antennas.

True-time delay beamforming based on photonic technologies has been extensively researched in the past few years and a large number of papers have been published [68]–[102]. The techniques reported in literature can be classified into two categories: true-time delay beamforming based on free-space optics and true-time delay beamforming based on fiber or guided-wave optics. In [77], a true-time delay beamforming system based on free space optics was proposed and experimentally demonstrated. Since the system was based on bulky optics, it has a large size and heavy weight. Most of the reported systems were implemented based fiber optics. The realization of tunable true-time delays based on a fiber-optic prism consisting of an array of dispersive delay lines was demonstrated in 1993 [71]. To reduce the size of the fiber-optic prism, the dispersive delay lines could be replaced by FBG delay lines [81]. A FBG prism consisting of five channels of FBG delay lines is shown in Fig. 30 [91]. As can be seen the beam pointing direction can be steered by simply tuning the wavelength of the tunable laser source. Since the grating spacing in the second delay line is very small, to simplify the fabrication, the discrete FBGs can be replaced by a single chirped Bragg grating. In fact, if all the discrete grating delay lines are replaced by chirped grating delay lines, a true time delay beamforming system with continuous beam steering would be realized [97].

The architecture shown in Fig. 30 has the advantage of using a single tunable laser source, which is easy to implement with fast beam steering capability by tuning the wavelength of the tunable laser source. However, the prism consists of many discrete FBGs, which may make the system bulky, complicated and unstable. A solution is to use a single chirped Bragg grating [80]. As shown in Fig. 31, a single wideband chirped Bragg grating is used. Different time delays are achieved by reflecting the wavelengths from a tunable multiwavelength laser source

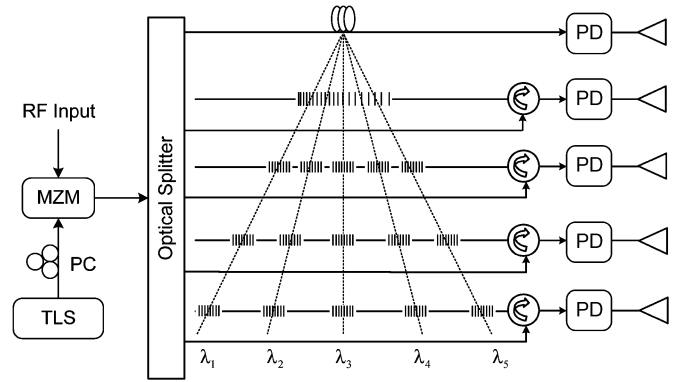


Fig. 30. A photonic true-time delay beamforming system based on a FBG prism.

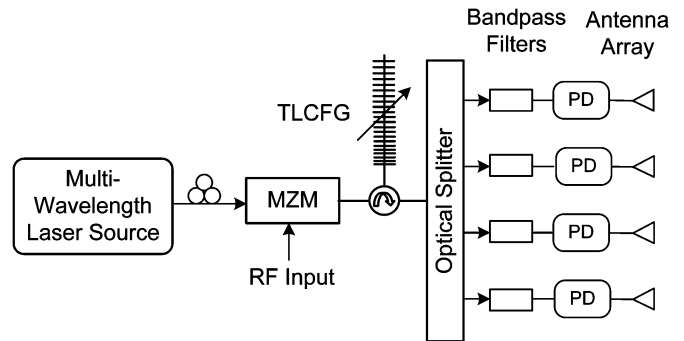


Fig. 31. A photonic true-time delay beamforming system using a chirped Bragg grating.

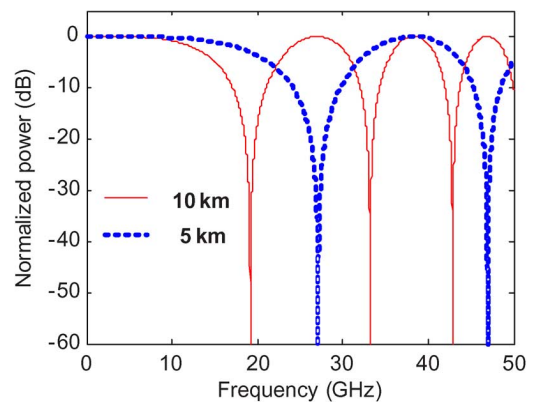


Fig. 32. Power distribution as a function of microwave frequency.

at different locations of the chirped Bragg grating. To achieve tunable time delays, the wavelength spacing should be tunable. Therefore, a multiwavelength laser source with tunable wavelength spacing is required [90]. To use a light source with fixed multi-wavelengths, recently we proposed to tune the chirp rate of the chirped Bragg grating [97]. A technique to tune the chirp rate of a chirped FBG without central wavelength shift was demonstrated in [100].

The two architectures shown in Figs. 30 and 31 only operate for one-dimensional beamforming. A few architectures have been proposed to achieve two-dimensional beamforming [77], [101], [102]. In [77], [101], a two-dimensional true-time delay beamforming system was demonstrated, with tunable time

delays achieved using free-space optical prisms and two-dimensional spatial light modulators. In [102], a two-dimensional true-time delay beamforming system based on pure fiber optic components with smaller size was demonstrated. The key module of the system is the delay-line matrix consisting of 2×2 optical micro-electromechanical (MEMS) switches with fiber-optic delay lines connected between cross ports. A 2-bit \times 4-bit optical true-time delay for a 10-GHz two-dimensional phased array antenna was implemented by cascading a wavelength-dependent true-time delay unit with a unit time delay of 12 ps in the x -direction and a wavelength-independent true-time delay unit with a unit time delay of 6 ps in the y -direction.

V. RADIO-OVER-FIBER SYSTEMS

The distribution of radio signals over optical fiber to take advantage of the low loss and broadband bandwidth of the state-of-the-art optical fibers has been a topic of interest for the last two decades with some radio-over-fiber systems deployed for practical applications. A radio-over-fiber system was experimentally demonstrated as early as in 1990 [103]. A four-channel second-generation cordless telephony signals were distributed over single-mode fiber by using subcarrier multiplexing. The subcarrier frequencies were located in a frequency band of 864–868 MHz. Multi-longitudinal-mode laser diodes operating at 1300 nm were used in the transmitter, which were directly modulated by the subcarriers. PIN photodetectors were employed at the receivers. This system exhibited an electrical dynamic range of 70 dB for one channel and 50 dB for four channels. Since then, numerous radio-over-fiber networks employing subcarrier multiplexing and wavelength division multiplexing were reported [104]–[107] with different network topologies such as star-tree [104]–[106] and ring [107], in which optical wavelength-division multiplexing was employed to increase the system capacity and to make the system to operate in a full-duplex mode.

To increase the data rate, radio-over-fiber system operating in the mm-wave band has been a topic of interest with numerous papers published in the last few years [108]–[113].

Radio-over-fiber systems operating in the conventional RF frequency bands for present wireless communication systems were also widely studied [114]–[120]. Radio-over-fiber systems based on multimode optical fibers with a reduced cost were also investigated [121]–[127]. Demonstrations of the co-existence of analog radio-over-fiber systems and digital fiber-to-the-home systems with dense wavelength division multiplexed technology were also reported in [128], [129].

Other techniques to develop subsystems for radio-over-fiber applications have also been extensively studied, which include remote optical generation of microwave and mm-wave signals [1]–[19], [130]–[137], optical up-conversion of a microwave signal [64]–[67], [138]–[142].

In a radio-over-fiber system, numerous issues should be addressed. In the following, we will discuss two of the most important issues, 1) Single-sideband modulation to combat fiber chromatic dispersion, and 2) The dynamic range of a radio-over-fiber link.

A. Single-Sideband Modulation

Due to the chromatic dispersion, double sideband modulation is not preferred in a radio-over-fiber system, especially for a transmission link operating at high microwave frequency and long distance, since the double-sideband-modulated microwave signal will suffer from the chromatic-dispersion-induced power penalty. The reason behind the microwave power fading along the fiber is due to the cancellation of the beat signal between the upper sideband and the carrier and the beat signal between the lower sideband and the carrier, since the optical carrier and the two sidebands will travel at different velocities, leading to the phase changes. For a radio-over-fiber link using an optical fiber with a length of L and a dispersion parameter of D , the power distribution as a function of microwave frequency is given by [143]

$$P_o \propto \cos^2 \left(\frac{\pi L D}{C} \lambda_C^2 f_{RF}^2 \right) \quad (13)$$

where λ_C is the wavelength of the optical carrier, f_{RF} is the microwave frequency, C is the velocity of light in vacuum.

Fig. 32 shows the power distribution of a double-sideband modulated signal in a single mode fiber of a length of 5 and 10 km. The fiber dispersion parameter is 17 ps/nm.km. Power fading due to the chromatic dispersion is observed.

Although the dispersion can be compensated in the optical domain using a length of dispersion compensating fiber or a chirped FBG, a cost-effective and commonly used approach is to use single sideband modulation. Numerous techniques have been proposed to implement single sideband modulation [143]–[146].

One well-known approach to achieving single sideband modulation is to use a dual-port Mach–Zehnder modulator, as shown in Fig. 33 [143]. An RF signal is applied to the two RF ports, with one being directly connected to the RF port and the other being phase shifted by 90° and then connected to the second RF port. The output signal will have the optical carrier and one optical sideband.

Single-sideband modulation can also be achieved by using an optical filter, such as an FBG, to filter out one of the two sidebands [144]. The major problem associated with the approach is that the optical filter should have a narrowband width to effectively suppress one of the sideband. For a RF signal operating a low frequency [a few gigahertz (GHz)], a regular uniform FBG can hardly fulfill this task due to the large bandwidth. Recently, we have demonstrated to use an ultra-narrow transmission band FBG to achieve single-sideband modulation [147]. The ultra-narrow transmission band FBG was designed and fabricated based on the equivalent phase shift technology [19].

B. Dynamic Range

One of the key performance measures that characterizes the performance of a radio-over-fiber link is the dynamic range. In a radio-over fiber system using direct modulation or external modulation, due to the modulation nonlinearity of a laser diode or the inherent nonlinearity of the transfer function of a Mach–Zehnder modulator, nonlinear distortions such as harmonic distortions and intermodulation distortions would be generated, which will limit the dynamic range of

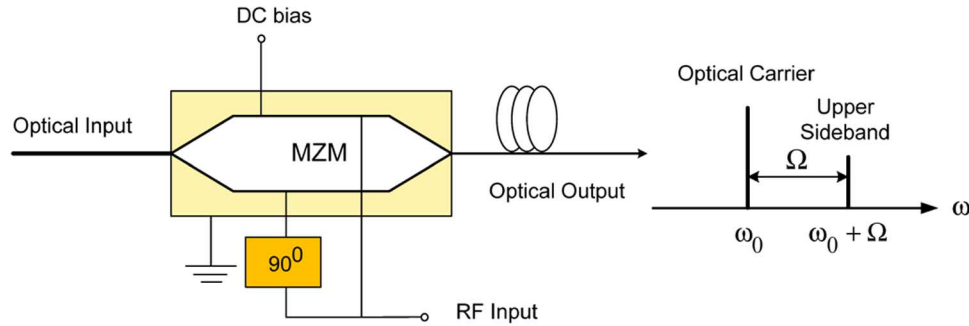


Fig. 33. Single-sideband modulation using a dual-port Mach-Zehnder modulator.

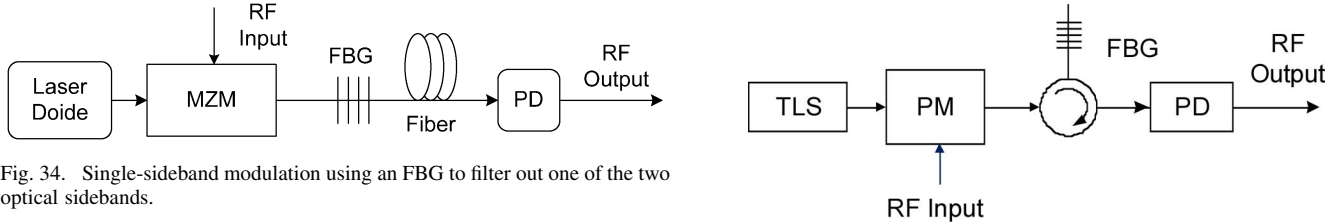


Fig. 34. Single-sideband modulation using an FBG to filter out one of the two optical sidebands.

the radio-over-fiber link. Numerous techniques have been proposed to combat the nonlinear distortions [148]–[154]. It was reported in [148] that the third-order inter-modulation can be minimized in a direct-modulation-based radio-over-fiber system by using an optimum bias current to the laser diode. The use of feed-forward linearization of a directly modulated laser diode would also provide a distortion cancellation [149]. The distortions of a laser diode can also be reduced by using predistortion [150]. For a radio-over-fiber system employing an external modulator, the nonlinear distortions caused by the Mach-Zehnder modulator can be reduced by techniques such as predistortion of the analog signals [151], [152] and linearization of the Mach-Zehnder modulator [153], [154].

In addition to the above techniques to reduce the nonlinear distortions, another solution to increase the dynamic range is to reduce the noise floor. It is known that a reduction of the noise floor in a radio-over-fiber link would increase the spurious-free dynamic range (SFDR). Spurious-free dynamic range is defined as the difference between the minimum signal that can be detected above the noise floor and the maximum signal that can be detected without distortions. In a radio-over-fiber link, the SFDR is limited by several noise sources, including the optical phase-induced intensity noise, shot noise and relative-intensity noise (RIN). For a radio-over-fiber link that uses independent light sources with very narrow linewidth, the phase-induced intensity noise is very small and can be neglected [155]. Therefore, the dominant noise sources are the shot noise and the RIN, both are associated with the average received optical power at the photodetector. The shot noise and the RIN powers are linearly and quadratically proportional to the received optical power. Therefore, a solution to increase the SFDR is to reduce the average received optical power. The reduction of shot noise and the RIN to improve the dynamic range of an radio-over-fiber link has been proposed recently, such as intensity-noise cancellation [156], optical carrier filtering [157], low-biasing of a Mach-Zehnder modulator [158]–[161], coherent detection [162], and optical phase modulation to intensity modulation (PM-IM) conversion using an FBG-based frequency discriminator [63].

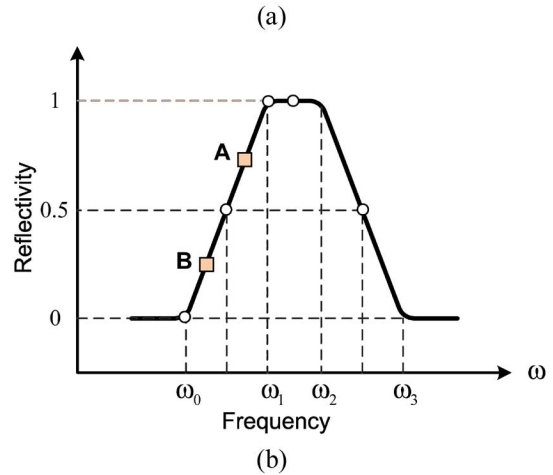


Fig. 35. Optical phase modulation to intensity modulation conversion using an FBG-based frequency discriminator. (a) The schematic of the system. (b) The reflection spectrum of the FBG.

As an example, in Fig. 35(a), we show a scheme to reduce the noise powers based on optical PM-IM conversion using an FBG-based frequency discriminator. Since the dc power decreases quadratically when the optical carrier is shifted closer to the bottom of the FBG spectrum while the signal power decreases linearly, the noise power is significantly decreased while maintaining a smaller decrease in the signal power [62]. This important property enables us to choose a reflection point closer to the bottom of the FBG spectrum, to substantially reduce the optical-power-induced noises with slightly sacrificing the signal power, leading to an increased SFDR. For example, in Fig. 35(b), if the optical carrier is shifted from A to B, the optical power is reduced by nine times, while the signal power is reduced by three times. Therefore, an improvement in SFDR of 5 dB is achieved [62].

VI. PHOTONICS ANALOG-TO-DIGITAL CONVERSION

Analog-to-digital conversion is an electronic process to convert a continuous-time signal to a digital signal without losing

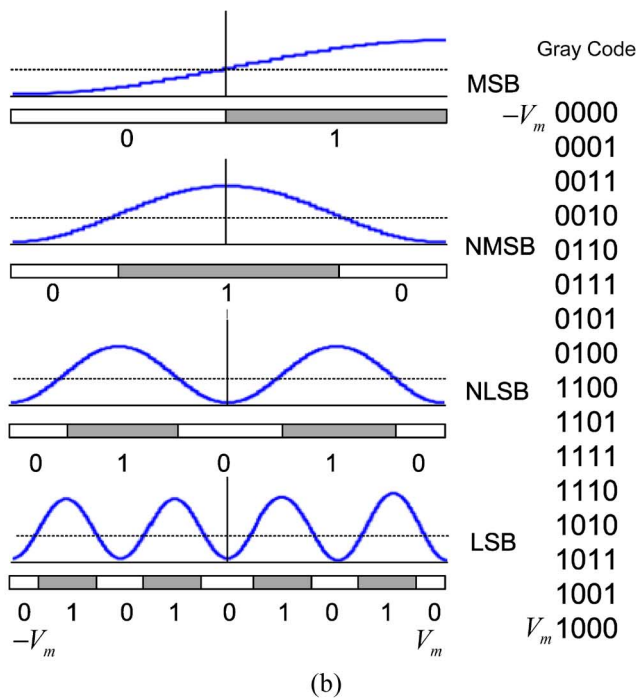
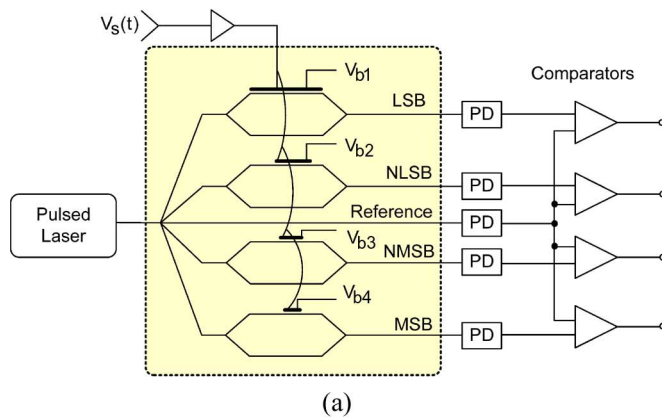


Fig. 36. A 4-bit analog-to-digital converter using an array of Mach-Zehnder modulators with each modulator having an electrode length that is twice that of its nearest more significant bit. (a) The schematic of the system, (b) Gray code produced at the outputs of the comparators.

any information, which is essential for many modern applications, such as wireless communications, radar, advanced instrumentation, and electronic warfare systems. Although there is a significant progress in analog-to-digital conversion, the sampling speed of the state-of-the-art electronics is still limited, which is the bottleneck that limits most of the modern applications where a fast analog-to-digital conversion is required. A comprehensive review on electronic analog-to-digital conversion can be found in [163].

In the last few decades, the use of optical technologies to achieve analog-to-digital conversion has attracted great interest thanks to the technological breakthrough in pulsed laser sources, which can produce ultra-narrow and high-repetition rate optical sampling pulses with a timing jitter significantly below that of electronic circuitry. In addition, the use of optical sampling would have an added advantage, that is, the back-coupling between the optical sampling pulses and the electrical signal being sampled is small and negligible. A comprehensive review on

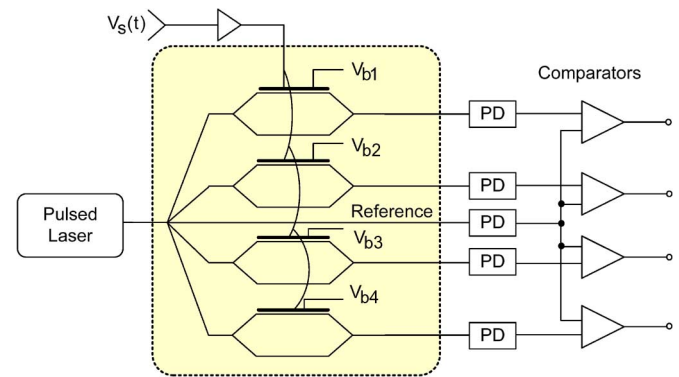


Fig. 37. An analog-to-digital converter using Mach-Zehnder modulators with identical half-wave voltages.

photonic analog-to-digital conversion has been recently published in [164].

Analog-to-digital conversion using photonic components was pioneered by a few researchers including the well-known approach proposed by Taylor [165], [166], with the architecture shown in Fig. 36(a). In the proposed system, an array of Mach-Zehnder modulators was used, with the input analog signal being symmetrically folded by the Mach-Zehnder modulators with each Mach-Zehnder modulator having an electrode length that is twice that of its nearest more significant bit (NMSB), leading to a doubled folding frequency, as shown in Fig. 36(b). The folding property in the transfer function imposes a requirement that the half-wave voltage of the Mach-Zehnder modulator at the least significant bit (LSB) should be very low, which is difficult to realize with currently available photonics technology.

To avoid using Mach-Zehnder modulators with very low half-wave voltages, a few modified system structures have been proposed [167], [168], including the use of cascaded Mach-Zehnder modulators with identical half-wave voltage [167] and cascaded phase modulators [168]. Recently, a scheme to use a free-space interferometric structure was proposed in which a phase modulator was incorporated in one arm of the interferometer [169], [170]. By placing the photodetectors at the specific locations of the diffraction pattern generated at the output of the interferometer, digital data with linear binary code are generated. The same concept was recently demonstrated in [171], but the interferometric structure was realized based on pure fiber-optics, which makes the system more compact.

Recently, a photonic analog-to-digital conversion scheme implemented using an array of Mach-Zehnder modulators with identical half-wave voltages was demonstrated [172]. The system architecture is identical to the one shown in Fig. 36(a), except that the Mach-Zehnder modulators have identical half-wave voltages, as shown in Fig. 37. The Mach-Zehnder modulators are biased such that the transfer functions of the Mach-Zehnder modulators are laterally shifted, which leads to the generation of a linear binary code to represent the analog input signal. The operation principle is shown in Fig. 38. For an analog-to-digital converter with four channels, the four Mach-Zehnder modulators are biased with their transfer functions shifted laterally with a uniform phase spacing of $\pi/4$, as shown in Fig. 38(a). The outputs from the comparators with a

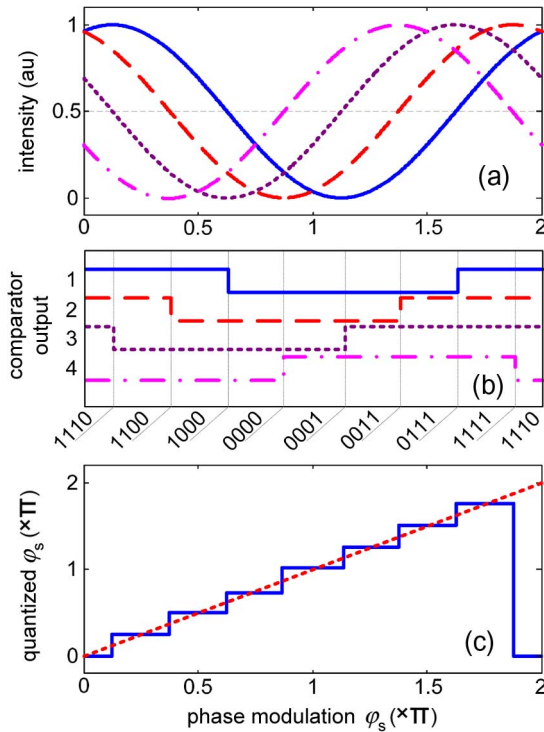


Fig. 38. The operation of a 4-channel photonic analog-to-digital converter using Mach-Zehnder modulators with identical half-wave voltages. (a) the transfer functions of the four Mach-Zehnder modulators; (b) *The linear binary code* at the outputs of the comparators; (c) quantized value (solid line) v.s. the input phase modulation (dotted line).

threshold level as half of the full scale are shown in Fig. 38(b). The quantized values of the signal at the output of the 4-channel analog-to-digital converter are shown in Fig. 38(c).

The use of the Mach-Zehnder modulators with identical half-wave voltages simplifies greatly the design and implementation, which provides a high potential for integration. The key limitation of the approach in [172] is that for an n -channel ADC, the code length of this scheme is $2n$, while the code length is 2^n for the schemes in [165], [166]. Note that the channel number n in this approach does not equal to the bit resolution N_R when n is greater than 2. The bit resolution N_R of the approach in [172] is given by $N_R = \log_2(2n)$. A solution to improve the bit resolution while using small channel number is to use multiple comparators for one channel [173].

VII. DISCUSSIONS AND CONCLUSION

Photonic techniques provide many advantageous features over its electronic counterpart for the generation, processing, control, and distribution of microwave and mm-wave signals for applications such as broadband wireless access networks, sensor networks, radar, satellite communications, instrumentation, and warfare systems. In this tutorial, an overview about the microwave photonics techniques developed in the last three decades was presented, with an emphasis on the system architectures for photonic generation and processing of microwave and mm-wave signals, photonic true-time delay beamforming, radio-over-fiber systems, and analog-to-digital conversion. The development status of microwave photonic devices has been recently reviewed in [174], which was not discussed

here. In addition to the four conventional topics reviewed in this tutorial, a few new topics would be of interest to the microwave photonics community, which includes photonic generation of arbitrary microwave and mm-wave waveforms [175], Ultra-wideband over fiber systems [176], and slow light for microwave photonics applications [177].

Different microwave photonics system architectures to realize different functionalities have been proposed. The key challenge in implementing these systems for practical applications is the large size and high cost of the systems. The microwave photonics systems demonstrated in the past few years were mainly based on discrete photonic and microwave components, which make the systems bulky, heavy and costly. A solution to the limitation is to use photonic integrated circuits. The current activities in silicon photonics [178] would have an important impact on the development and implementation of future microwave photonics systems if a major breakthrough in developing practical silicon lasers is envisaged in the near future.

ACKNOWLEDGMENT

A large number of papers have been published in the area of microwave photonics in the past few years. Due to the limited space, only a limited number of papers were cited in this tutorial. The author would like to acknowledge the contributions of the colleagues in the area.

The author would also like to acknowledge the following people from the Microwave Photonics Research Laboratory of the University of Ottawa for their assistance: S. Blais, H. Chi, Y. Dai, G. Qi, H. Rideout, Q. Wang, Y. Yan, and F. Zeng.

REFERENCES

- [1] U. Gliese, T. N. Nielsen, S. Nørskov, and K. E. Stubkjaer, "Multifunctional fiber-optic microwave links based on remote heterodyne detection," *IEEE Trans. Microw. Theory Tech.*, vol. 46, no. 5, pp. 458–468, May 1998.
- [2] L. Goldberg, H. F. Taylor, J. F. Weller, and D. M. Bloom, "Microwave signal generation with injection locked laser diodes," *Electron. Lett.*, vol. 19, no. 13, pp. 491–493, Jun. 1983.
- [3] L. Goldberg, A. Yurek, H. F. Taylor, and J. F. Weller, "35 GHz microwave signal generation with injection locked laser diode," *Electron Lett.*, vol. 21, no. 18, pp. 714–715, Aug. 1985.
- [4] J. Harrison and A. Mooradian, "Linewidth and offset frequency locking of external cavity GaAlAs lasers," *IEEE J. Quantum Electron.*, vol. 25, no. 6, pp. 1252–1255, Jun. 1989.
- [5] R. T. Ramos and A. J. Seeds, "Fast heterodyne optical phase-lock loop using double quantum well laser diodes," *Electron. Lett.*, vol. 28, no. 1, pp. 82–83, Jan. 1992.
- [6] U. Gliese, T. N. Nielsen, M. Bruun, E. L. Christensen, K. E. Stubkjaer, S. Lindgren, and B. Broberg, "A wideband heterodyne optical phase-lock loop for generation of 3–18 GHz microwave carriers," *IEEE Photon. Technol. Lett.*, vol. 4, no. 8, pp. 936–938, Aug. 1992.
- [7] A. C. Bordonalli, C. Walton, and A. J. Seeds, "High-Performance phase locking of wide linewidth semiconductor lasers by combined use of optical injection locking and optical phase-lock loop," *J. Lightw. Technol.*, vol. 17, no. 2, pp. 328–342, Feb. 1999.
- [8] K. J. Williams, "6–34 GHz offset phase locking of Nd: YAG 1319 nm nonplanar ring lasers," *Electron. Lett.*, vol. 25, no. 18, pp. 1242–1243, Aug. 1989.
- [9] Z. F. Fan and M. Dagenais, "Optical generation of a mHz-linewidth microwave signal using semiconductor lasers and a discriminator-aided phase-locked loop," *IEEE Trans. Microw. Theory Tech.*, vol. 45, no. 8, pp. 1296–1300, Aug. 1997.
- [10] H. Rideout, J. Seregelyi, S. Paquet, and J. P. Yao, "Discriminator-aided optical phase-lock loop incorporating a frequency down-conversion module," *IEEE Photon. Technol. Lett.*, vol. 18, no. 22, pp. 2344–2346, Nov. 2006.

- [11] A. C. Bordonalli, C. Walton, and A. J. Seeds, "High-performance phase locking of wide linewidth semiconductor lasers by combined use of optical injection locking and optical phase-lock loop," *J. Lightw. Technol.*, vol. 17, no. 2, pp. 328–342, Feb. 1999.
- [12] J. J. O'Reilly, P. M. Lane, R. Heidemann, and R. Hofstetter, "Optical generation of very narrow linewidth millimeter wave signals," *Electron. Lett.*, vol. 28, no. 25, pp. 2309–2311, 1992.
- [13] J. J. O'Reilly and P. M. Lane, "Remote delivery of video services using mm-wave and optics," *J. Lightw. Technol.*, vol. 12, no. 2, pp. 369–375, Feb. 1994.
- [14] J. J. O'Reilly and P. M. Lane, "Fiber-supported optical generation and delivery of 60 GHz signals," *Electron. Lett.*, vol. 30, no. 16, pp. 1329–1330, 1994.
- [15] P. Shen, N. J. Gomes, P. A. Davies, W. P. Shillue, P. G. Huggard, and B. N. Ellison, "High-purity millimeter-wave photonic local oscillator generation and delivery," in *Proc. Int. Microw. Photonics Topical Meeting*, Sep. 10–12, 2003, pp. 189–192.
- [16] G. Qi, J. P. Yao, J. Seregelyi, C. Bélisle, and S. Paquet, "Generation and distribution of a wide-band continuously tunable mm-wave signal with an optical external modulation technique," *IEEE Trans. Microw. Theory Tech.*, vol. 53, no. 10, pp. 3090–3097, Oct. 2005.
- [17] G. Qi, J. P. Yao, J. Seregelyi, C. Bélisle, and S. Paquet, "Optical generation and distribution of continuously tunable millimeter-wave signals using an optical phase modulator," *J. Lightw. Technol.*, vol. 23, no. 9, pp. 2687–2695, Sep. 2005.
- [18] X. Chen, Z. Deng, and J. P. Yao, "Photonic generation of microwave signal using a dual-wavelength single-longitudinal-mode fiber ring laser," *IEEE Trans. Microw. Theory Tech.*, vol. 54, no. 2, pp. 804–809, Feb. 2006.
- [19] X. Chen, J. P. Yao, and Z. Deng, "Ultrathin dual-transmission-band fiber Bragg grating filter and its application in a dual-wavelength single-longitudinal-mode fiber ring laser," *Opt. Lett.*, vol. 30, no. 16, pp. 2068–2070, Aug. 2005.
- [20] K. Wilner and A. P. Va den Heuvel, "Fiber-optic delay lines for microwave signal processing," *Proc. IEEE*, vol. 64, no. 5, pp. 805–807, May 1976.
- [21] E. C. Heyd and R. A. Minasian, "A solution to the synthesis problem of recirculating optical delay line filter," *IEEE Photon. Technol. Lett.*, vol. 6, no. 7, pp. 833–835, Jul. 1994.
- [22] J. Capmany, J. Cascon, J. L. Martín, S. Sales, D. Pastor, and J. Martí, "Synthesis of fiber-optic delay line filters," *J. Lightw. Technol.*, vol. 13, no. 10, pp. 2003–2012, Oct. 1995.
- [23] J. Capmany and J. Martín, "Solutions to the synthesis problem of optical delay line filters," *Opt. Lett.*, vol. 20, no. 23, pp. 2438–2440, Dec. 1995.
- [24] D. B. Hunter and R. Minasian, "Reflectivity tapped fiber optic transversal filter using in-fiber Bragg gratings," *Electron. Lett.*, vol. 31, no. 12, pp. 1010–1012, Jun. 1995.
- [25] D. B. Hunter and R. Minasian, "Microwave optical filters using in-fiber Bragg grating arrays," *IEEE Microw. Guided Wave Lett.*, vol. 6, no. 2, pp. 103–105, Feb. 1996.
- [26] D. B. Hunter and R. Minasian, "Photonic signal processing of microwave signals using an active-fiber Bragg-grating-pair structure," *IEEE Trans. Microw. Theory Tech.*, vol. 45, no. 8, pp. 1463–1466, Aug. 1997.
- [27] J. Martí, F. Ramos, and R. I. Laming, "Photonic microwave filter employing multimode optical sources and wideband chirped fiber gratings," *Electron. Lett.*, vol. 34, no. 18, pp. 1760–1761, Sep. 1998.
- [28] J. Capmany, D. Pastor, and B. Ortega, "New and flexible fiber-optic delay-line filters using chirped Bragg gratings and laser arrays," *IEEE Trans. Microw. Theory and Technol.*, vol. 47, no. 7, pp. 1321–1326, Jul. 1999.
- [29] J. Martí, V. Polo, F. Ramos, and D. Moodie, "Photonics tunable microwave filters employing electro-absorption modulators and wideband chirped fiber gratings," *Electron. Lett.*, vol. 35, no. 4, pp. 305–306, Feb. 1999.
- [30] G. Yu, W. Zhang, and J. A. R. Williams, "High-performance microwave transversal filter using fiber Bragg grating arrays," *IEEE Photon. Technol. Lett.*, vol. 12, no. 9, pp. 1183–1185, Sep. 2000.
- [31] D. Pastor, J. Capmany, and B. Ortega, "Broad-band tunable microwave transversal notch filter based on tunable uniform fiber Bragg gratings as slicing filters," *IEEE Photon. Technol. Lett.*, vol. 13, no. 7, pp. 726–728, Jul. 2001.
- [32] W. Zhang, J. A. R. Williams, and I. Bennion, "Polarization synthesized optical transversal filter employing high birefringence fiber gratings," *IEEE Photon. Technol. Lett.*, vol. 13, no. 5, pp. 523–525, May. 2001.
- [33] D. Pastor, J. Capmany, and B. Ortega, "Experimental demonstration of parallel fiber-optic-based RF filtering using WDM techniques," *IEEE Photon. Technol. Lett.*, vol. 12, no. 1, pp. 77–78, Jan. 2000.
- [34] V. Polo, B. Vidal, J. L. Corral, and J. Martí, "Novel tunable photonics microwave filter based on laser arrays and $N \times N$ AWG-based delay lines," *IEEE Photon. Technol. Lett.*, vol. 15, no. 4, pp. 584–586, Apr. 2003.
- [35] T. A. Cusick, S. Iezekiel, R. E. Miles, S. Sales, and J. Capmany, "Synthesis of all-optical microwave filters using Mach-Zehnder lattices," *IEEE Trans. Microw. Theory Tech.*, vol. 45, no. 8, pp. 1458–1462, Aug. 1997.
- [36] D. Norton, S. Johns, C. Keefer, and R. Soref, "Tunable microwave filtering using high dispersion fiber time delays," *IEEE Photon. Technol. Lett.*, vol. 6, no. 7, pp. 831–832, Jul. 1994.
- [37] K. H. Lee, W. Y. Choi, S. Choi, and K. Oh, "A novel tunable fiber-optic microwave filter using multimode DCF," *IEEE Photon. Technol. Lett.*, vol. 15, no. 7, pp. 969–971, Jul. 2003.
- [38] J. Capmany, B. Ortega, and D. Pastor, "A tutorial on microwave photonic filters," *J. Lightw. Technol.*, vol. 24, no. 1, pp. 201–229, Jan. 2006.
- [39] R. A. Minasian, "Photonic signal processing of microwave signals," *IEEE Trans. Microw. Theory Tech.*, vol. 54, no. 2, pp. 832–846, Feb. 2006.
- [40] S. Sales, J. Capmany, J. Martí, and D. Pastor, "Experimental demonstration of fiber-optic delay line filters with negative coefficients," *Electron. Lett.*, vol. 31, no. 13, pp. 1095–1096, Jun. 1995.
- [41] F. Coppinger, S. Yegnanarayanan, P. D. Trinh, and B. Jalali, "All-optical RF filter using amplitude inversion in a semiconductor optical amplifier," *IEEE Trans. Microw. Theory Tech.*, vol. 45, no. 8, pp. 1473–1477, Aug. 1997.
- [42] T. Mukai, K. Inoue, and T. Saitoh, "Homogeneous gain saturation in 1.5 m InGaAsP traveling-wave semiconductor laser amplifiers," *Appl. Phys. Lett.*, vol. 51, no. 6, pp. 381–383, Aug. 1987.
- [43] X. Wang and K. T. Chan, "Tunable all-optical incoherent bipolar delay-line filter using injection-locked Fabry-Perot laser and fiber Bragg gratings," *Electron. Lett.*, vol. 36, no. 24, pp. 2001–2002, Nov. 2000.
- [44] S. Li, K. S. Chiang, W. A. Gambling, Y. Liu, L. Zhang, and I. Bennion, "A novel tunable all-optical incoherent negative-tap fiber-optical transversal filter based on a DFB laser diode and fiber Bragg gratings," *IEEE Photon. Technol. Lett.*, vol. 12, no. 9, pp. 1207–1209, Sep. 2000.
- [45] J. Mora, M. V. Andres, J. L. Cruz, B. Ortega, J. Capmany, D. Pastor, and S. Sales, "Tunable all-optical negative multitap microwave filters based on uniform fiber Bragg gratings," *Opt. Lett.*, vol. 28, no. 15, pp. 1308–1310, Aug. 2003.
- [46] J. Capmany, D. Pastor, A. Martínez, B. Ortega, and S. Sales, "Microwave photonics filter with negative coefficients based on phase inversion in an electro-optic modulator," *Opt. Lett.*, vol. 28, no. 16, pp. 1415–1417, Aug. 2003.
- [47] B. Vidal, J. L. Corral, and J. Martí, "All-optical WDM multi-tap microwave filter with flat bandpass," *Opt. Express*, vol. 14, no. 2, pp. 581–586, Jan. 2006.
- [48] F. Zeng, J. Wang, and J. P. Yao, "All-optical microwave bandpass filter with negative coefficients based on a phase modulator and linearly chirped fiber Bragg gratings," *Opt. Lett.*, vol. 30, no. 17, pp. 2203–2205, Sep. 2005.
- [49] J. Wang, F. Zeng, and J. P. Yao, "All-optical microwave bandpass filter with negative coefficients based on PM-IM conversion," *IEEE Photon. Technol. Lett.*, vol. 17, no. 10, pp. 2176–2178, Oct. 2005.
- [50] J. P. Yao and Q. Wang, "Photonic microwave bandpass filter with negative coefficients using a polarization modulator," *IEEE Photon. Technol. Lett.*, vol. 19, no. 9, pp. 644–646, May 2007.
- [51] Q. Wang and J. P. Yao, "Multi-tap photonic microwave filters with arbitrary positive and negative coefficients using a polarization modulator and an optical polarizer," *IEEE Photon. Technol. Lett.*, vol. 20, no. 2, pp. 78–80, Jan. 2008.
- [52] N. You and R. A. Minasian, "A novel tunable microwave optical notch filter," *IEEE Trans. Microw. Theory Tech.*, vol. 49, no. 10, pt. 2, pp. 2002–2005, Oct. 2001.
- [53] A. Loayssa, J. Capmany, M. Sagues, and J. Mora, "Demonstration of incoherent microwave photonic filters with all-optical complex coefficients," *IEEE Photon. Technol. Lett.*, vol. 18, no. 16, pp. 1744–1746, Aug. 2006.
- [54] Y. Yan and J. P. Yao, "A tunable photonic microwave filter with a complex coefficient using an optical RF phase shifter," *IEEE Photon. Technol. Lett.*, vol. 19, no. 19, pp. 1472–1474, Sep. 2007.

- [55] A. Loayssa, R. Hernandez, D. Benito, and S. Galech, "Characterization of stimulated Brillouin scattering spectra by use of optical single-sideband modulation," *Opt. Lett.*, vol. 29, no. 6, pp. 638–640, Mar. 2004.
- [56] Y. Dai and J. P. Yao, "Nonuniformly-spaced photonic microwave delay-line filter," *Opt. Express*, vol. 16, no. 7, pp. 4713–4718, Mar. 2008.
- [57] F. Zeng and J. P. Yao, "All-optical bandpass microwave filter based on an electro-optic phase modulator," *Optics Express*, vol. 12, no. 16, pp. 3814–3819, Aug. 2004.
- [58] F. Zeng and J. P. Yao, "Investigation of phase modulator based all-optical bandpass microwave filter," *J. Lightw. Technol.*, vol. 23, no. 4, pp. 1721–1728, Apr. 2005.
- [59] Y. Dai and J. P. Yao, "Microwave pulse phase encoding using a photonic microwave delay-line filter," *Opt. Lett.*, vol. 32, no. 24, pp. 3486–3488, Dec. 2007.
- [60] Y. Dai and J. P. Yao, "Chirped RF pulse generation using a photonic microwave filter with a quadratic phase response," *IEEE Photon. Technol. Lett.*, to be published.
- [61] B. Cabon, Y. Le Guennec, M. Lourdiane, and G. Maury, "Photonic mixing in RF modulated optical links," in *LEOS 2006*, Oct. 2006, pp. 408–409.
- [62] Y. Yan and J. P. Yao, "Photonic microwave bandpass filter with improved dynamic range," *Opt. Lett.*, to be published.
- [63] J. Zhang and T. E. Darcie, "Low-biased microwave-photonic link using optical frequency or phase modulation and fiber-Bragg-grating discriminator," presented at the Optical Fiber Commun. Conf., Anaheim, CA, 2006, paper OWG1, unpublished.
- [64] F. Zeng and J. P. Yao, "All-optical microwave mixing and bandpass filtering in a radio-over-fiber link," *IEEE Photon. Technol. Lett.*, vol. 17, no. 4, pp. 899–901, April 2005.
- [65] J. Yao, J. P. Yao, Z. Deng, and J. Liu, "Investigation of room-temperature multiwavelength fiber-ring laser that incorporates an SOA-based phase modulator in the laser cavity," *J. Lightw. Technol.*, vol. 23, no. 8, pp. 2484–2490, Aug. 2005.
- [66] J. P. Yao, G. Maury, Y. L. Guennec, and B. Cabon, "All-optical sub-carrier frequency conversion using an electrooptic phase modulator," *IEEE Photon. Technol. Lett.*, vol. 17, no. 11, pp. 2427–2429, Nov. 2005.
- [67] Y. Le Guennec, G. Maury, J. P. Yao, and B. Cabon, "New optical microwave up-conversion solution in radio-over-fiber networks for 60 GHz wireless applications," *J. Lightw. Technol.*, vol. 24, no. 3, pp. 1277–1282, Mar. 2006.
- [68] W. Ng, A. A. Walston, G. L. Tansonan, J. J. Lee, I. L. Newberg, and N. Bernstein, "The first demonstration of an optically steered microwave phased array antenna using true-time-delay," *J. Lightw. Technol.*, vol. 9, no. 9, pp. 1124–1131, Sep. 1991.
- [69] R. D. Esman, J. J. Monsma, J. L. Dexter, and D. G. Cooper, "Microwave true time-delay modulator using fibre-optic dispersion," *Electron. Lett.*, vol. 28, no. 20, pp. 1905–1908, Sep. 1992.
- [70] P. M. Freitag and S. R. Forrest, "A coherent optically controlled phased array antenna system," *IEEE Microw. Guided Wave Lett.*, vol. 3, no. 9, pp. 293–295, Sep. 1993.
- [71] R. D. Esman, M. Y. Frankel, J. L. Dexter, L. Goldberg, M. G. Parent, D. Stilwell, and D. G. Cooper, "Fiber-optic prism true time-delay antenna feed," *IEEE Photon. Technol. Lett.*, vol. 5, no. 11, pp. 1347–1349, Nov. 1993.
- [72] G. A. Ball, W. H. Glenn, and W. W. Morey, "Programmable fiber optic delay line," *IEEE Photon. Technol. Lett.*, vol. 6, no. 6, pp. 741–743, Jun. 1994.
- [73] E. H. Monsay, K. C. Baldwin, and M. J. Caccuitto, "Photonic true time delay for high-frequency phased array systems," *IEEE Photon. Technol. Lett.*, vol. 6, no. 1, pp. 118–120, Jan. 1994.
- [74] A. Molony, C. Edge, and I. Bennion, "Fibre grating time delay element for phased array antennas," *Electron. Lett.*, vol. 31, no. 17, pp. 1485–1486, Aug. 1995.
- [75] I. Frigyes and A. J. Seeds, "Optically generated true-time delay in phased-array antennas," *IEEE Trans. Microw. Theory Tech.*, vol. 43, no. 9, pp. 2378–2386, Sep. 1995.
- [76] L. Xu, R. Taylor, and S. R. Forrest, "The use of optically coherent detection techniques for true-time delay phased array and systems," *J. Lightw. Technol.*, vol. 13, no. 8, pp. 1663–1678, Aug. 1995.
- [77] D. Dolfi, F. Michel-Gabriel, S. Bann, and J. P. Huignard, "Two-dimensional optical architecture for time-delay beam forming in a phased-array antenna," *Opt. Lett.*, vol. 16, no. 4, pp. 255–257, Feb. 1991.
- [78] L. Xu, R. Taylor, and S. R. Forrest, "True time-delay phased-array antenna feed system based on optical heterodyne techniques," *IEEE Photon. Technol. Lett.*, vol. 8, no. 1, pp. 160–162, Jan. 1996.
- [79] A. Molony, Z. Lin, J. A. R. Williams, I. Bennion, C. Edge, and J. Fells, "Fiber Bragg-grating true time-delay systems: Discrete-grating array 3-b delay lines and chirped-grating 6-b delay lines," *IEEE Trans. Microw. Theory Tech.*, vol. 45, no. 8, pp. 1527–1530, Aug. 1997.
- [80] J. L. Corral, J. Marti, J. M. Fuster, and R. I. Laming, "True time-delay scheme for feeding optically controlled phased-array antennas using chirped-fiber gratings," *IEEE Photon. Technol. Lett.*, vol. 9, no. 11, pp. 1529–1531, Nov. 1997.
- [81] H. Zmuda, R. A. Soref, P. Payson, S. Johns, and E. N. Toughlian, "Photonic beamformer for phased array antennas using a fiber grating prism," *IEEE Photon. Technol. Lett.*, vol. 9, no. 2, pp. 241–243, Feb. 1997.
- [82] R. A. Minasian and K. E. Alameh, "Optical-fiber-grating-based beamforming network for microwave phased arrays," *IEEE Trans. Microw. Theory Tech.*, vol. 45, no. 8, pp. 1513–1517, Aug. 1997.
- [83] P. J. Matthews, M. Y. Frankel, and R. D. Esman, "A wide-band fiber-optic true-time-steered array receiver capable of multiple independent simultaneous beams," *IEEE Photon. Technol. Lett.*, vol. 10, no. 5, pp. 722–724, May 1998.
- [84] D. T. K. Tong and M. C. Wu, "Multiwavelength optically controlled phased-array antennas," *IEEE Trans. Microw. Theory Tech.*, vol. 46, no. 1, pp. 108–115, Jan. 1998.
- [85] D. T. K. Tong and M. C. Wu, "Common transmit/receive module for multiwavelength optically controlled phased array antennas," in *Optical Fiber Commun. Conf. and Exhibit*, Feb. 1998, pp. 354–355.
- [86] D. Dolfi, D. Mongardien, S. Tonda, M. Schaller, and J. Chazelas, "Photonics for airborne phased array radars," in *IEEE Int. Conf. on Phased Array Systems and Technology*, May 2000, pp. 379–382.
- [87] B. Ortega, J. L. Cruz, J. Capmany, M. V. Andrés, and D. Pastor, "Variable delay line for phased-array antenna based on a chirped fiber grating," *IEEE Trans. Microw. Theory Tech.*, vol. 48, no. 8, pp. 1352–1360, Aug. 2000.
- [88] B. Ortega, J. L. Cruz, J. Capmany, M. V. Andrés, and D. Pastor, "Analysis of a microwave time delay line based on a perturbed uniform fiber Bragg grating operating at constant wavelength," *J. Lightw. Technol.*, vol. 18, no. 3, pp. 430–436, Mar. 2000.
- [89] Y. Wang, S. C. Tjin, J. Yao, J. P. Yao, L. He, and K. A. Ngoi, "Wavelength-switching fiber laser for optically controlled phased-array antenna," *Opt. Comm.*, vol. 211, no. 1–6, pp. 147–151, Oct. 2002.
- [90] J. P. Yao, J. Yang, and Y. Liu, "Continuous true-time-delay beamforming employing a multiwavelength tunable fiber laser source," *IEEE Photon. Technol. Lett.*, vol. 14, no. 5, pp. 687–689, May 2002.
- [91] Y. Liu, J. P. Yao, and J. Yang, "Wideband true-time-delay unit for phased array beamforming using discrete-chirped fiber grating prism," *Opt. Comm.*, vol. 207, no. 1–6, pp. 177–187, Jun. 2002.
- [92] B. Vidal, D. Madrid, J. L. Corral, V. Polo, A. Martinez, J. Hendrik den Besten, F. Soares, J. Marti, and M. K. Smit, "Photonic true-time delay beamformer for broadband wireless access network at 40 GHz band," in *IEEE MTT-S Int. Microw. Symp. Dig.*, Jun. 2002, vol. 3, pp. 1949–1952.
- [93] S. T. Winnall and D. B. Hunter, "A fibre Bragg grating based scanning receiver for electronic warfare applications," in *Int. Topical Meeting on Microw. Photonics*, Jan. 2002, pp. 211–214.
- [94] Y. Liu, J. Yang, and J. P. Yao, "Continuous true-time-delay beamforming for phased array antenna using a tunable chirped fiber grating delay line," *IEEE Photon. Technol. Lett.*, vol. 14, no. 8, pp. 1172–1174, Aug. 2002.
- [95] Y. Chen and R. T. Chen, "A fully packaged true time delay module for a K-band phased array antenna system demonstration," *IEEE Photon. Technol. Lett.*, vol. 14, no. 8, pp. 1175–1177, Aug. 2002.
- [96] R. Rotman, O. Raz, and M. Tur, "Requirements for true time delay imaging systems with photonic components," in *IEEE Int. Symp. on Phased Array Systems and Technology*, Oct. 2003, pp. 193–198.
- [97] Y. Liu and J. P. Yao, "Wideband true time-delay beamformer employing a tunable chirped fiber grating prism," *Appl. Opt.*, vol. 42, no. 13, pp. 2273–2277, May 2003.
- [98] O. Raz, R. Rotman, Y. Danziger, and M. Tur, "Implementation of photonic true time delay using high-order-mode dispersion compensating fibers," *IEEE Photon. Technol. Lett.*, vol. 16, no. 5, pp. 1367–1369, May 2004.
- [99] S. S. Lee, Y. H. Oh, and S. Y. Shin, "Photonic microwave true-time delay based on a tapered fiber Bragg grating with resistive coating," *IEEE Photon. Technol. Lett.*, vol. 16, no. 10, pp. 2335–2337, Oct. 2004.

- [100] Y. Liu, J. P. Yao, X. Dong, and J. Yang, "Tunable chirping of a fibre Bragg grating without center wavelength shift using simply supported beam," *Opt. Eng.*, vol. 41, no. 4, pp. 740–741, Apr. 2002.
- [101] D. Dolfi, P. Joffre, J. Antoine, J. P. Huignard, D. Philippet, and P. Granger, "Experimental demonstration of a phased-array antenna optically controlled with phase and time delays," *Appl. Opt.*, vol. 35, no. 26, pp. 5293–5300, Sep. 1996.
- [102] B. M. Jung, J. D. Shin, and B. G. Kim, "Optical true time-delay for two-dimensional X-band phased array antennas," *IEEE Photon. Technol. Lett.*, vol. 19, pp. 877–879, Jun. 2007.
- [103] A. J. Cooper, "Fiber/radio for the provision of cordless/mobile telephony services in the access network," *Electron. Lett.*, vol. 26, no. 24, pp. 2054–2056, Nov. 1990.
- [104] G. H. Smith, D. Novak, and C. Lim, "A millimeter-wave full-duplex radio-over-fiber star-tree architecture incorporating WDM and SCM," *IEEE Photon. Tech. Lett.*, vol. 10, no. 11, pp. 1650–1652, Nov. 1998.
- [105] A. Nkansah, A. Das, N. J. Gomes, P. Shen, and D. Wake, "VCSEL-based single-mode and multimode fiber star/tree distribution network for millimeter-wave wireless systems," in *Proc. Microw. Photonics*, Oct. 2006, pp. 1–4.
- [106] A. Kaszubowska, P. Anandarajah, and L. P. Barry, "Multifunctional operation of a fiber Bragg grating in a WDM/SCM radio over fiber distribution system," *IEEE Photon. Tech. Lett.*, vol. 16, no. 2, pp. 605–607, Feb. 2004.
- [107] A. Stöhr, K. Kitayama, and D. Jäger, "Full-duplex fiber-optic RF sub-carrier transmission using a dual-function modulator/photodetector," *IEEE Trans. Microw. Theory Tech.*, vol. 47, no. 7, pp. 1338–1341, Jul. 1999.
- [108] H. Ogawa, D. Polifko, and S. Banba, "Millimeter-wave fiber optics systems for personal radio communication," *IEEE Trans. Microw. Theory Tech.*, vol. 40, no. 12, pp. 2285–2293, Dec. 1992.
- [109] M. Goloubkoff, E. Penard, D. Tanguy, P. Legaud, D. Mathoorasing, F. Devaux, and C. Minot, "Outdoor and indoor applications for broadband local loop with fibre supported mm-wave radio systems," in *Tech. Dig. IEEE MTT-S Int. Microw. Symp.*, Jun. 1997, vol. 1, pp. 31–34.
- [110] L. Noel, D. Wake, D. G. Moodie, D. D. Marcenac, L. D. Westbrook, and D. Nasset, "Novel techniques for high-capacity 60 GHz radio-over-fiber transmission systems," *IEEE Trans. Microw. Theory Tech.*, vol. 45, no. 8, pp. 1416–1423, Aug. 1997.
- [111] K. Kitayama, T. Kuri, and Y. Ogawa, "Error-free optical 156-Mbit/s millimeter-wave wireless transport through 60-GHz external modulation," in *OFC '98 Tech. Dig.*, Feb. 1998, pp. 14–15.
- [112] J. J. V. Olmos, T. Kuri, and K. Kitayama, "Dynamic reconfigurable WDM 60-GHz millimeter-waveband radio-over-fiber access network: Architectural considerations and experiment," *J. Lightw. Technol.*, vol. 25, no. 11, pp. 3374–3380, Nov. 2007.
- [113] A. Nkansah, A. Das, N. J. Gomes, and P. Shen, "Multilevel modulated signal transmission over serial single-mode and multimode fiber links using vertical-cavity surface-emitting lasers for millimeter-wave wireless communications," *IEEE Trans. Microw. Theory Tech.*, vol. 55, no. 6, pp. 1219–1228, Jun. 2007.
- [114] B. L. Dang and I. Niemegeers, "Analysis of IEEE 802.11 in radio over fiber home networks," in *IEEE Conf. on Local Computer Networks*, Nov. 2005, pp. 744–747.
- [115] Y. Horiuchi, "ROF application to 3G mobile systems in offices and outdoors," in *Proc. Microw. Photonics*, Oct. 2005, p. 3-3.
- [116] M. J. Crisp, L. Sheng, A. Wonfor, R. V. Penty, and I. H. White, "Demonstration of a radio over fibre distributed antenna network for combined in-building WLAN and 3G coverage," in *OFC/NFOEC 2007*, Mar. 2007, pp. 1–3.
- [117] A. Brizido, M. Lima, R. Nogueira, P. Andre, and A. Teixeira, "3G radio distribution based on directly modulated lasers over passive transparent optical networks," in *Microw. and Optoelectronics Conf.*, 2007, pp. 658–661.
- [118] H. Kosek, Y. He, X. Gu, and X. N. Fernando, "All-optical demultiplexing of WLAN and cellular CDMA radio signals," *J. Lightw. Technol.*, vol. 25, no. 6, pp. 1401–1409, Jun. 2007.
- [119] M. J. Crisp, L. Sheng, A. Watts, R. V. Penty, and I. H. White, "Up-link and downlink coverage improvements of 802.11g signals using a distributed antenna network," *J. Lightw. Technol.*, vol. 25, no. 11, pp. 3388–3395, Nov. 2007.
- [120] M. Mjeku and N. J. Gomes, "Performance analysis of 802.11e transmission bursting in fiber-fed networks," in *Radio and Wireless Symp.*, Jan. 2008, pp. 133–136.
- [121] C. Lethien, J.-P. Vilcot, S. McMurtry, J.-F. Lampin, D. Vignaud, P. Miska, D. Decoster, and F. Mollot, "Characterisation of SiO₂ transferred GaAs electroabsorption modulator for 850 nm radio over fibre systems based on multimode fibre," *Electron. Lett.*, vol. 40, no. 17, pp. 1075–1076, Aug. 2004.
- [122] C. Loyez, C. Letien, N. Deparis, J. P. Vilcot, D. Decoster, N. Rolland, and P. A. Rolland, "A radio over multimode system based on a LO phase-noise cancellation for 60-GHz WLAN," in *European Microw. Conf.*, Oct. 2005, vol. 1, pp. 3–6.
- [123] A. Nkansah and N. J. Gomes, "Characterization of radio over multimode fiber links using coherence bandwidth," *IEEE Photon. Tech. Lett.*, vol. 17, no. 12, pp. 2694–2696, Dec. 2005.
- [124] A. Nkansah, A. Das, C. Lethien, J.-P. Vilcot, N. J. Gomes, I. J. Garcia, J. C. Batohelhor, and D. Wake, "Simultaneous dual band transmission over multimode fiber-fed indoor wireless network," *IEEE Microw. Wireless Compon. Lett.*, vol. 16, no. 11, pp. 627–629, Nov. 2006.
- [125] J. D. Ingham, R. V. Penty, and I. H. White, "Bidirectional multimode-fiber communication links using dual-purpose vertical-cavity devices," *J. Lightw. Technol.*, vol. 24, no. 3, pp. 1283–1294, Mar. 2006.
- [126] I. Gasulla and J. Capmany, "Transmission of high-frequency radio over fibre signals through short and middle reach multimode fibre links using a low-linewidth laser," in *Proc. Microw. Photonics*, Oct. 2007, pp. 116–119.
- [127] M. Sauer, A. Kobayakov, and J. George, "Radio over fiber for picocellular network architectures," *J. Lightw. Technol.*, vol. 25, no. 11, pp. 3301–3320, Nov. 2007.
- [128] K. Kitayama, T. Kuri, H. Toda, and J. J. V. Olmos, "Radio over fiber: DWDM analog/digital access network and its enabling technologies," in *Lasers and Electro-Optics Society, LEOS 2007*, Oct. 2007, pp. 794–795.
- [129] T. Kuri, H. Toda, and K. Kitayama, "Radio over fiber: DWDM-based analog/digital access networking and its enabling technologies," in *Radio and Wireless Symp.*, Jan. 2008, pp. 137–140.
- [130] R. Gindera and D. Jager, "Remote optoelectronic microwave generation in fiber radio systems using a ring oscillator," in *European Microw. Conf.*, Sep. 2006, pp. 1115–1117.
- [131] C. Lin, W. Peng, P. Peng, C. Chiang, J. Chen, B. Chiou, and S. Chi, "Simultaneous baseband and RF signal generation using only one single-electrode MZM based on double-sideband with optical carrier suppression," in *Proc. Microw. Photonics*, Oct. 2006, pp. 1–4.
- [132] J. Yu, Z. Jia, L. Yi, Y. Su, G. Chang, and T. Wang, "Optical millimeter-wave generation or up-conversion using external modulators," *IEEE Photon. Tech. Lett.*, vol. 18, no. 1, pp. 265–267, Jan. 2006.
- [133] Z. Deng and J. P. Yao, "Photonic generation of microwave signal using a rational harmonic mode-locked fiber ring laser," *IEEE Trans. Microw. Theory Tech.*, vol. 54, no. 2, pp. 763–767, Feb. 2006.
- [134] J. Yu, Z. Jia, L. Xu, L. Chen, T. Wang, and G. Chang, "DWDM optical millimeter-wave generation for radio-over-fiber using an optical phase modulator and an optical interleaver," *IEEE Photon. Tech. Lett.*, vol. 18, no. 13, pp. 1418–1420, Jul. 2006.
- [135] M. Mohamed, X. Zhang, B. Hraimel, and K. Wu, "Efficient photonic generation of millimeter-waves using optical frequency multiplication in radio-over-fiber systems," in *Proc. Microw. Photonics*, Oct. 2007, pp. 179–182.
- [136] J. Zhang, H. Chen, M. Chen, T. Wang, and S. Xie, "A photonic microwave frequency quadrupler using two cascaded intensity modulators with repetitive optical carrier suppression," *IEEE Photon. Tech. Lett.*, vol. 19, no. 14, pp. 1057–1059, Jul. 2007.
- [137] J. Yu, Z. Jia, T. Wang, and G. Chang, "Centralized lightwave radio-over-fiber system with photonic frequency quadrupling for high-frequency millimeter-wave generation," *IEEE Photon. Tech. Lett.*, vol. 19, no. 19, pp. 1499–1501, Oct. 2007.
- [138] H.-J. Song, J. S. Lee, and J.-I. Song, "All-optical frequency upconversion of radio over fibre signal with optical heterodyne detection," *Electron. Lett.*, vol. 40, no. 5, pp. 330–331, Mar. 2004.
- [139] J. S. Lee, H.-J. Song, W. B. Kim, M. Fujise, Y.-H. Kim, and J.-I. Song, "All-optical harmonic frequency upconversion of radio over fibre signal using cross-phase modulation in semiconductor optical amplifier," *Electron. Lett.*, vol. 40, no. 19, pp. 1211–1213, Sep. 2004.
- [140] H. Song, J. S. Lee, and J. Song, "Simultaneous all-optical frequency upconversion for WDM radio over fiber applications," in *Tech. Dig. IEEE MTT-S Int. Microw. Symp.*, Jun. 2005, p. 4.
- [141] M. Shin and P. Kumar, "1.25 Gbps optical data channel up-conversion in 20 GHz-band via a frequency-doubling optoelectronic oscillator for radio-over-fiber systems," in *Tech. Dig. IEEE MTT-S Int. Microw. Symp.*, Jun. 2007, pp. 63–66.

- [142] J. P. Yao and H. Chi, "Frequency quadrupling and upconversion in a radio over fiber link," *J. Lightw. Technol.*, vol. 26, no. 15, Aug. 2008.
- [143] G. H. Smith, D. Novak, and Z. Ahmed, "Overcoming chromatic-dispersion effects in fiber-wireless systems incorporating external modulators," *IEEE Trans. Microw. Theory Tech.*, vol. 45, no. 8, pp. 1410–1415, Aug. 1997.
- [144] J. Park, W. V. Sorin, and K. Y. Lau, "Elimination of the fibre chromatic dispersion penalty on 1550 nm millimeter-wave optical transmission," *Electron. Lett.*, vol. 33, no. 6, pp. 512–513, Mar. 1997.
- [145] M. Attygalle, C. Lim, G. J. Pendock, A. Nirmalathas, and G. Edvell, "Transmission improvement in fiber wireless links using fiber Bragg gratings," *IEEE Photon. Technol. Lett.*, vol. 17, no. 1, pp. 190–192, Jan. 2005.
- [146] Y. Shen, X. Zhang, and K. Chen, "Optical single sideband modulation of 11-GHz RoF system using stimulated Brillouin scattering," *IEEE Photon. Technol. Lett.*, vol. 17, no. 6, pp. 1277–1279, Jun. 2005.
- [147] S. Blais and J. P. Yao, "Optical single sideband modulation using an ultranarrow dual-transmission-band fiber Bragg grating," *IEEE Photon. Technol. Lett.*, vol. 18, no. 21, pp. 2230–2232, Nov. 2006.
- [148] S. Yaalob, W. R. Wan Abdullah, M. N. Osman, A. K. Zamzuri, R. Mohamad, M. R. Yahya, A. F. Awang Mat, M. R. Mokhtar, and H. A. Abdul Rashid, "Effect of laser bias current to the third order intermodulation in the radio over fibre system," in *RF and Microw. Conf.*, Sep. 2006, pp. 444–447.
- [149] D. Hassin and R. Vahldieck, "Feedforward linearization of analog modulated laser diodes—Theoretical analysis and experimental verification," *IEEE Trans. Microw. Theory Tech.*, vol. 41, no. 12, pp. 2376–2382, Dec. 1993.
- [150] L. Roselli, V. Borgioni, F. Zepparelli, F. Ambrosi, M. Comez, P. Faccin, and A. Casini, "Analog laser predistortion for multiservice radio-over-fiber systems," *J. Lightw. Technol.*, vol. 21, no. 5, pp. 1211–1223, May 2003.
- [151] A. Katz, W. Jemison, M. Kubak, and J. Dragone, "Improved radio over fiber performance using predistortion linearization," in *IEEE MTT-S Int. Microw. Symp. Dig.*, Philadelphia, PA, Jun. 2003, pp. 1403–1406.
- [152] V. Magoon and B. Jalali, "Electronic linearization and bias control for externally modulated fiber optic link," in *IEEE Int. Microw. Photon. Meeting*, Oxford, U.K., Sep. 2000, pp. 145–147.
- [153] J. H. Schaffner and W. B. Bridges, "Inter-modulation distortion in high dynamic range microwave fiber-optic links with linearized modulators," *J. Lightw. Technol.*, vol. 11, no. 1, pp. 3–6, Jan. 1993.
- [154] E. I. Ackerman, "Broad-band linearization of a Mach-Zehnder electrooptic modulator," *IEEE Trans. Microw. Theory Tech.*, vol. 47, no. 12, pp. 2271–2279, Dec. 1999.
- [155] S. Yamamoto, N. Edagawa, H. Taga, Y. Yoshida, and H. Wakabayashi, "Analysis of laser phase noise to intensity noise conversion by chromatic dispersion in intensity modulation and direct detection optical-fiber transmission," *J. Lightw. Technol.*, vol. 8, no. 11, pp. 1716–1722, Nov. 1990.
- [156] S. Mathai, F. Cappelluti, T. Jung, D. Novak, R. B. Waterhouse, D. Siveco, A. Y. Cho, G. Ghione, and M. C. Wu, "Experimental demonstration of a balanced electroabsorption modulated microwave photonic link," *IEEE Trans. Microw. Theory Tech.*, vol. 49, no. 10, pp. 1956–1961, Oct. 2001.
- [157] R. D. Esman and K. J. Williams, "Wideband efficiency improvement of fiber optic systems by carrier subtraction," *IEEE Photon. Technol. Lett.*, vol. 7, no. 2, pp. 218–220, Feb. 1995.
- [158] T. E. Darcie and P. F. Driessen, "Class-AB Techniques for high-dynamic-range microwave photonic links," *IEEE Photon. Technol. Lett.*, vol. 18, no. 8, pp. 929–931, Apr. 2006.
- [159] L. T. Nichols, K. J. Williams, and R. D. Esman, "Optimizing the ultra-wide-band photonic link," *IEEE Trans. Microw. Theory Tech.*, vol. 45, no. 8, pp. 1384–1389, Aug. 1997.
- [160] M. L. Farwell, W. S. C. Chang, and D. R. Huber, "Increased linear dynamic range by low biasing the Mach-Zehnder modulator," *IEEE Photon. Technol. Lett.*, vol. 5, no. 7, pp. 779–782, Jul. 1999.
- [161] T. E. Darcie, A. Moye, P. F. Driessen, J. D. Bull, H. Kato, and N. A. F. Jaeger, "Noise reduction in class-AB microwave-photonic links," in *Int. Topical Meeting on Microw. Photonics*, Seoul, South Korea, 2005, pp. 329–332.
- [162] C. Lindsay, "An analysis of coherent carrier suppression for photonic microwave links," *IEEE Trans. Microw. Theory Tech.*, vol. 47, no. 7, pp. 1194–1200, Jul. 1999.
- [163] R. H. Walden, "Analog-to-digital converter survey and analysis," *IEEE J. Sel. Areas Commun.*, vol. 17, no. 4, pp. 539–550, Apr. 1999.
- [164] G. C. Valley, "Photonic analog-to-digital converters," *Opt. Express*, vol. 15, no. 5, pp. 1955–1982, Mar. 2007.
- [165] H. F. Taylor, "An electrooptic analog-to-digital converter," *Proc. IEEE*, vol. 63, no. 10, pp. 1524–1525, Oct. 1975.
- [166] H. F. Taylor, "An optical analog-to-digital converter-design and analysis," *IEEE J. Quantum Electron.*, vol. 15, no. 4, pp. 210–216, Apr. 1979.
- [167] B. Jalali and Y. M. Xie, "Optical folding-flash analog-to-digital converter with analog encoding," *Opt. Lett.*, vol. 20, no. 18, pp. 1901–1903, Sep. 1995.
- [168] M. Currie, "Optical quantization of microwave signals via distributed phase modulation," *J. Lightw. Technol.*, vol. 23, no. 2, pp. 827–833, Feb. 2005.
- [169] J. Stigwall and S. Galt, "Interferometric analog-to-digital conversion scheme," *IEEE Photon. Technol. Lett.*, vol. 17, no. 2, pp. 468–470, Feb. 2005.
- [170] J. Stigwall and S. Galt, "Demonstration and analysis of a 40-Gigasample/s interferometric analog-to-digital converter," *J. Lightw. Technol.*, vol. 24, no. 3, pp. 1247–1256, Mar. 2006.
- [171] W. Li, H. Zhang, Q. Wu, Z. Zhang, and M. Yao, "All-optical analog-to-digital conversion based on polarization-differential interference and phase modulation," *IEEE Photon. Technol. Lett.*, vol. 19, no. 8, pp. 625–627, Apr. 2007.
- [172] H. Chi and J. P. Yao, "A photonic analog-to-digital conversion scheme using Mach-Zehnder modulators with identical half-wave voltages," *Opt. Express*, vol. 16, no. 2, pp. 567–572, Jan. 2008.
- [173] P. E. Pace and D. Styer, "High-resolution encoding process for an integrated optical analog-to-digital converter," *Opt. Eng.*, vol. 33, no. 8, pp. 2638–2645, Aug. 1994.
- [174] A. J. Seeds and K. J. Williams, "Microwave photonics," *J. Lightw. Technol.*, vol. 24, no. 12, pp. 4628–4641, Dec. 2006.
- [175] H. Chi and J. P. Yao, "All-fiber chirped microwave pulse generation based on spectral shaping and wavelength-to-time conversion," *IEEE Trans. Microw. Theory Tech.*, vol. 55, no. 9, pp. 1958–1963, Sep. 2007.
- [176] J. P. Yao, F. Zeng, and Q. Wang, "Photonic generation of ultra-wide-band signals," *J. Lightw. Technol.*, vol. 25, no. 11, pp. 3219–3235, Nov. 2007.
- [177] C. J. Chang-Hasnain and S. L. Chuang, "Slow and fast light in semiconductor quantum-well and quantum-dot devices," *J. Lightw. Technol.*, vol. 24, no. 12, pp. 4642–4654, Dec. 2006.
- [178] B. Jalali and S. Fathpour, "Silicon photonics," *J. Lightw. Technol.*, vol. 24, no. 12, pp. 4600–4615, Dec. 2006.



Jianping Yao (M'99–SM'01) received the Ph.D. degree in electrical engineering in 1997 from the Université de Toulon, Toulon, France.

He joined the School of Information Technology and Engineering, University of Ottawa, Ottawa, Canada, in 2001, where he is currently a Professor, Director of the Microwave Photonics Research Laboratory, and Director of the Ottawa-Carleton Institute for Electrical and Computer Engineering. From 1999 to 2001, he held a faculty position with the School of Electrical and Electronic Engineering,

Nanyang Technological University, Singapore. He holds a Yongqian Endowed Visiting Chair Professorship with Zhejiang University, China. He spent three months as an invited professor in the Institut National Polytechnique de Grenoble, France, in 2005. His research has focused on microwave photonics, which includes all-optical microwave signal processing, photonic generation of microwave, mm-wave and THz, radio over fiber, UWB over fiber, fiber Bragg gratings for microwave photonics applications, and optically controlled phased array antenna. His research interests also include fiber lasers, fiber-optic sensors and bio-photonics. He has authored or co-authored over 110 papers in refereed journals and over 100 papers in conference proceeding.

Dr. Yao received the 2005 International Creative Research Award of the University of Ottawa. He was the recipient of the 2007 George S. Gliniski Award for Excellence in Research. He was named University Research Chair in Microwave Photonics in 2007. He was a recipient of an NSERC Discovery Accelerator Supplements award in 2008. He is a Registered Professional Engineer in the Province of Ontario, Canada. He is a member of SPIE, OSA, IEEE/LEOS and IEEE/MTT societies. He is an Associate Editor of the *International Journal of Microwave and Optical Technology*. He is on the Editorial Board of *IEEE TRANSACTIONS ON MICROWAVE THEORY AND TECHNIQUES*